AERODYNAMIC ANALYSIS OF THE SOLID PROPELLANT BOOSTER DECELERATION SUBSYSTEM DROP TESTS

(NASA-CR-170670) AERODYNAMIC ANALYSIS OF THE SOLID PROPELLANT BOOSTER DECELERATION SUBSYSTEM DROP TESTS Final Report (Northrop Services, Inc., Huntsville, Ala.) 62 p
N83-70686
Unclas
00/20 01428

DEC 1982
RECEIVED
NASA STI FACILITY
ACCESS DEPT.

Submitted To:

NATIONAL AERONAUTICS AND SPACE ADMINISTRATION
GEORGE C. MARSHALL SPACE FLIGHT CENTER
Science and Engineering Directorate

Under Contract NAS8–32811

DEC 1982
RECEIVED
NASA STI FACILITY
ACQ BRANCH

Submitted By:

NORTHROP SERVICES, INC.
P. O. BOX 1484 Huntsville, Alabama 35807 (205) 837-0580

TR–230–1942

AERODYNAMIC ANALYSIS OF THE SOLID PROPELLANT BOOSTER DECELERATION SUBSYSTEM DROP TESTS

November 1978

by

L. R. Utreja

Prepared for:

NATIONAL AERONAUTICS AND SPACE ADMINISTRATION
GEORGE C. MARSHALL SPACE FLIGHT CENTER
Under Contract NAS8–32811

Reviewed and approved by:

W. W. Boyle

W W. Boyle, Manager
Aeromechanics

M. A. Sloan Jr

M A Sloan, Jr , Manager
Technology

NORTHROP SERVICES, INC.
P. O. BOX 1484
HUNTSVILLE, ALABAMA 35807
(205) 837-0580

FOREWORD

This technical report presents the work performed under Contract NAS8-32811, including alterations in scope authorized as an extension to the original contract. The work was performed for the Systems Dynamics Laboratory of the Marshall Space Flight Center. Technical contact was maintained through Mr. David L. Bacchus of the Aerodynamics Analysis Branch, ED-32.

TABLE OF CONTENTS

Section	Title	Page
	FOREWORD	ii
	LIST OF ILLUSTRATIONS	iv
	LIST OF TABLES	v
	NOMENCLATURE	vi
I	INTRODUCTION	1-1
II	DROP TEST DESCRIPTION	2-1
III	SRB REENTRY FLIGHT AND DTV DROP TEST ENVIRONMENTS	3-1
IV	DROP TEST ANALYSIS	4-1
	4.1 TERMINAL DRAG PERFORMANCE	4-1
	4.2 REEFED DRAG PERFORMANCE	4-3
	4.3 PARACHUTE FILLING TIMES	4-6
	4.4 PARACHUTE DEPLOYMENT DYNAMICS	4-8
V	CONCLUSIONS	5-1
VI	RECOMMENDATIONS	6-1
VII	REFERENCES	7-1

LIST OF ILLUSTRATIONS

Figure	Title	Page
2-1	DROP TEST VEHICLE (DTV)	2-3
2-2	SOLID ROCKET BOOSTER (SRB)	2-4
2-3	THE DTV AND THE SRB OUTLINES	2-5
2-4	MAIN PARACHUTE GEOMETRY	2-6
2-5	DROGUE AND PILOT PARACHUTE GEOMETRY	2-7
3-1	DSS DYNAMIC PRESSURE HISTORY FOR NOMINAL DESCENT	3-4
4-1	TERMINAL DRAG COEFFICIENT OF THE DSS PARACHUTES	4-11
4-2	INTERFERENCE FREE DRAG PERFORMANCE OF 20-DEGREE CONICAL RIBBON PARACHUTES	4-12
4-3	DROGUE PARACHUTE DRAG LOSS DUE TO FOREBODY INTERFERENCE	4-13
4-4	PARACHUTE DRAG LOSS AS A FUNCTION OF TRAILING DISTANCE AND FOREBODY DIAMETER	4-14
4-5	COMPARISON OF DROP TEST WITH PREDICTED DSS PARACHUTES DRAG OCEFFICIENT	4-15
4-6	REEFED DRAG COEFFICIENT OF THE DSS PARACHUTES	4-16
4-7	SINGLE CHUTE REEFED DRAG COEFFICIENT	4-17
4-8	EFFECT OF REEFING ON INTERFERENCE FREE DRAG CHARACTERISTICS OF 20-DEGREE CONICAL RIBBON PARACHUTE	4-18
4-9	MAIN CHUTES CLUSTER REEFED DRAG COEFFICIENT	4-19
4-10	REEFED MAIN CHUTES CLUSTER EFFICIENCY FACTOR	4-20
4-11	FILLING TIME OF DSS PARACHUTES VERSUS NONDIMENSIONAL REEFING LINE LENGTH	4-21
4-12	FILLING TIME OF DSS PARACHUTES VERSUS VELOCITY	4-22
4-13	NONDIMENSIONAL FILLING TIME OF THE DSS PARACHUTES	4-23
4-14	DAD-1 DROGUE 1st REEF AREA BUILDUP	4-24
4-15	DAD-1 DROGUE PARACHUTE AREA BUILDUP	4-25
4-16	DAD-1 MAIN PARACHUTES AREA BUILDUP	4-26
4-17	DAD-1 TOTAL MAIN PARACHUTES AREA BUILDUP	4-27
4-18	DAD-2 DROGUE AREA BUILDUP	4-28
4-19	DAD-2 MAIN PARACHUTE AREA BUILDUP TO 1st REEF	4-29
4-20	DAD-4 DROGUE AREA BUILDUP CURVE	4-30
4-21	DAD-6 DROGUE CHUTE AREA BUILDUP	4-31
4-22	DAD-6 MAIN CHUTE AREA BUILDUP	4-32

LIST OF TABLES

Table	Title	Page
3-1	AIR DROP TEST OBJECTIVES.	3-5
3-2	AIR DROP TEST SUMMARY	3-6
3-3	AIR DROP TEST CONDITIONS.	3-7
4-1	TERMINAL DRAG PERFORMANCE OF THE DSS PARACHUTES	4-2
4-2	REEFED DRAG PERFORMANCE OF THE DSS PARACHUTES	4-5
4-3	PARACHUTE FILLING TIMES	4-8

NOMENCLATURE

Symbol	Definition
a_T	Tangential acceleration (m/sec^2)
C_D	Drag coefficient of a parachute
C_DS	Drag area of a parachute (m^2)
$(C_DS)_v$	Drag area of the DTV or frustum (m^2)
D_o	Parachute nominal diameter (m)
g	Gravitational acceleration (9.81 m/sec^2)
K	Nondimensional filling time
L_R	Length of reefing line (m)
L_S	Length of suspension lines (m)
n	Total vehicle acceleration (no. of g's)
q	Dynamic pressure (N/m^2)
V_Z	Vertical component of velocity (m/sec)
V_T	Total velocity (m/sec)
W	Total system weight (kg)
x	Parachute trailing distance
V_{BS}	Velocity at the start of parachute inflation (m/sec)
ρ	Air density (kg/m^3)
ψ	Parachute drag area, C_DS
ΔD	Difference between parachute reefed diameters at the end and the start of inflation (m)

Section I

INTRODUCTION

Two solid rocket boosters (SRB's) will be used for each space shuttle flight to provide a major percentage of the initial ascent thrust. The SRB's, at burnout, will be separated from the External Tank at an altitude of approximately 46 kilometers. Each SRB weighs about 72,660 kg at burnout and will be recovered under unique conditions of high angle of attack and dynamic pressure. Each SRB has a Deceleration Subsystem (DSS) to control its attitude and terminally water impact at a velocity of about 26 m per sec.

The SRB DSS is comprised of a pilot chute, a drogue chute for attitude control, and three main parachutes for final descent and required terminal velocity. All of the parachutes are 20-degree conical ribbon parachutes with a geometric porosity of 16 percent.

The SRB parachutes design studies were initiated under a compressed time and cost effective schedule. Under these constraints it became imperative to investigate the existing data on 20-degree conical ribbon parachutes. The study was then supplemented by two NASA sponsored wind tunnel tests on scaled SRB parachute configurations. The test results (References 1, 2, and 3) provided parachute performance and the drogue chute deployment characteristics. The steady state drag test results and the available data base were used to estimate drag performance (Ref. 4) of the selected SRB parachute configurations. Another wind tunnel test was conducted on the scaled SRB nose cap under the expected drogue chute deployment conditions. The test results (Ref. 5) provided estimates of the nose cap ejection velocity requirements for clean separation. The full scale nose cap rocket sled tests (Ref. 6) were conducted to further verify the nose cap separation and initial phase of the drogue parachute deployment under the SRB designed environment of dynamic pressure and angle of attack.

The Development Air Drops (DAD's) were conducted to gather data on prototype parachutes under simulated flight environment. The drop test program started in June 1977 and was completed in September 1978. The objective of

the drop test program was to evaluate the parachute deployment process, parachute performance, and parachutes structural integrity under simulated SRB flight environment.

The purpose of this report is to present the results of the drop tests and assess aerodynamic performance of the SRB DSS based on these tests. The report also presents anomalies observed in the tests, correlations between wind tunnel tests and drop tests, and conclusions. However, no attempt is made here to determine tolerance levels on the estimated parachute performance.

Section II

DROP TEST DESCRIPTION

Six DAD's were performed at the National Parachute Test Range, El Centro, California. To accomplish the tests a Drop Test Vehicle (DTV) was used. The DTV (Figure 2-1) weighed less than one-third of the weight of the SRB (Figure 2-2). The DTV simulated a portion of the SRB frustum to allow sufficient ground clearance when mounted on the drop aircraft. The frustum was then tapered to a ballast cylindrical section through a flare section. The relative size of the DTV in relation to the SRB is presented in Figure 2-3.

The parachutes used were flight prototype parachutes. The main parachute is a 35m diameter, 96-gore, ribbon chute of uniform 16 percent porosity. A schematic of the main parachute cluster is shown in Figure 2-4. Each pair of the 96 suspension lines connects to one leg of a dispersion bridle, each bridle having six legs. The eight dispersion bridles are connected to eight risers that are connected in groups of fours to the two deck fittings that carry loads from each parachute into the structure.

The drogue parachute is a 16.46m diameter, 60-gore, ribbon chute of uniform 16 percent porosity. The 60 suspension lines are gathered, in groups of 5, to 12 suspension line groups that are attached to fittings on the upper deck of the frustum. The pilot parachute is a 3.5m diameter, 16-gore, ribbon chute of uniform 16 percent porosity. The parachute will be packed in a deployment bag that rests on top of the drogue chute pack, and is attached to the nose cap by an energy absorbing bridle. The pilot chute suspension lines converge to a single riser that is attached to the drogue chute deployment bag. Figure 2-5 shows the basic geometry of the drogue chute and the pilot chute.

In addition, there were DTV test peculiar parachutes. The DTV parachutes were the 3.5m diameter nose cap extraction chute and a 0.6m diameter vane parachute used in conjunction with the interim nose cap. A complete description of the DTV and the DSS parachutes is given in reference 7.

The instrumentation consisted of load cells to measure the drogue chute riser forces and the main parachute(s) riser forces, accelerometers to measure vehicle component accelerations, rate gyros, and motion picture cameras including vehicle-to-air, air-to-air, and ground-to-air cameras.

The space position data were obtained from cinetheodolites. These data were smoothed and corrected with meteorological data. The space position data was combined with Mach number and pressure to obtain dynamic pressure. The telemetered accerometer responses were filtered and transformed to the vehicle c.g., and the individual load cell data were summed to obtain total parachute load. The motion picture films were used to determine the sequence of events in the drop test, the parachute area build up curves, and the parachute canopy shapes. The parachute filling times were also obtained from film data.

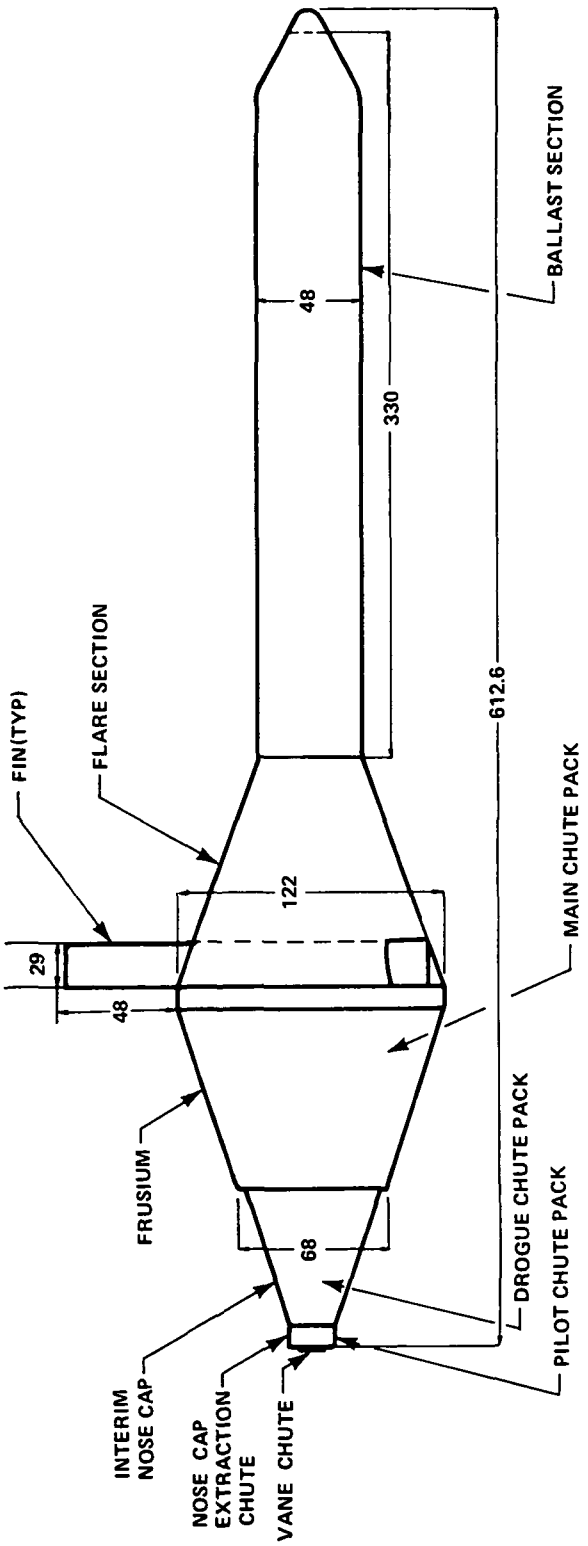

Figure 2-1. DROP TEST VEHICLE (DTV)

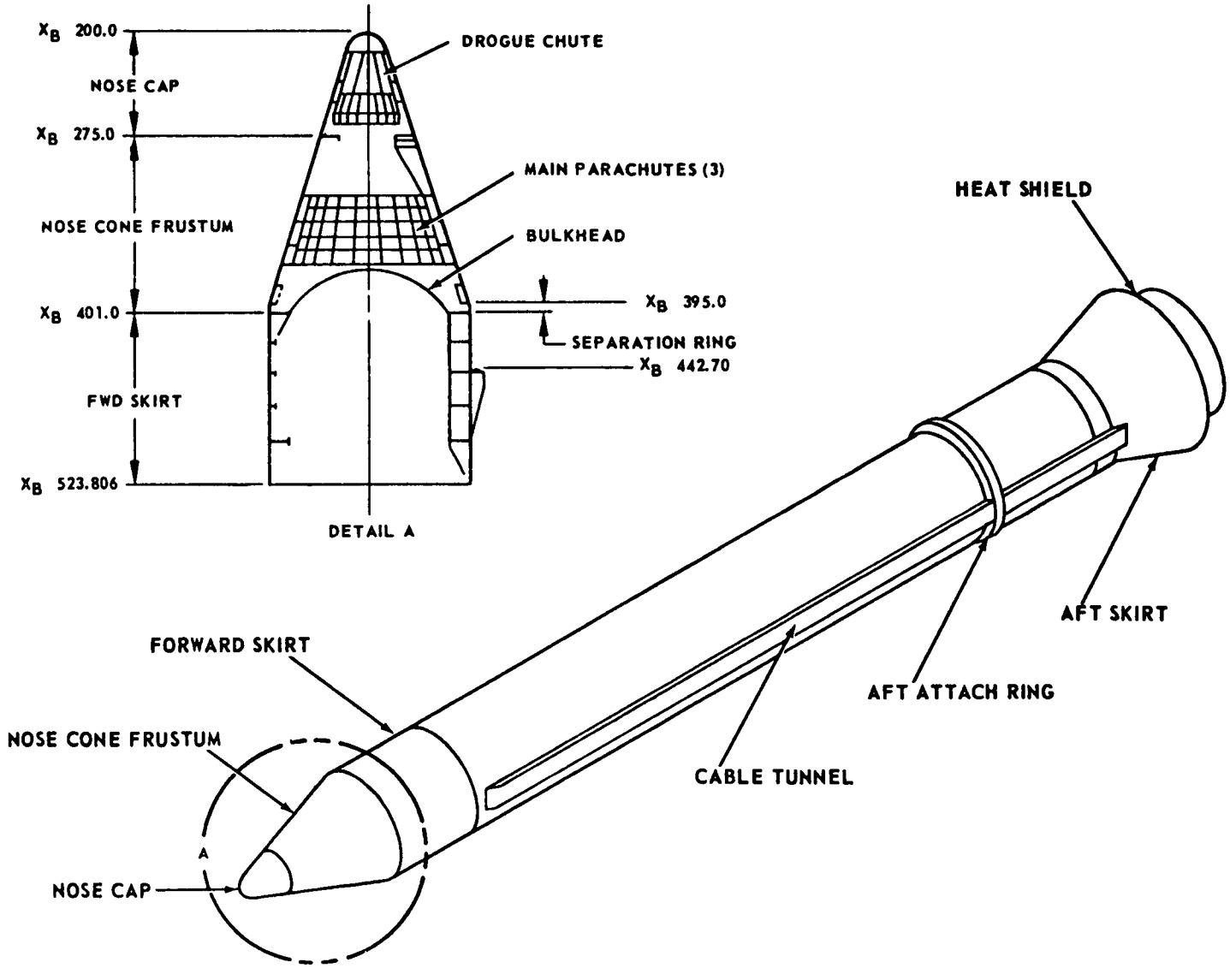

Figure 2-2. SOLID ROCKET BOOSTER (SRB)

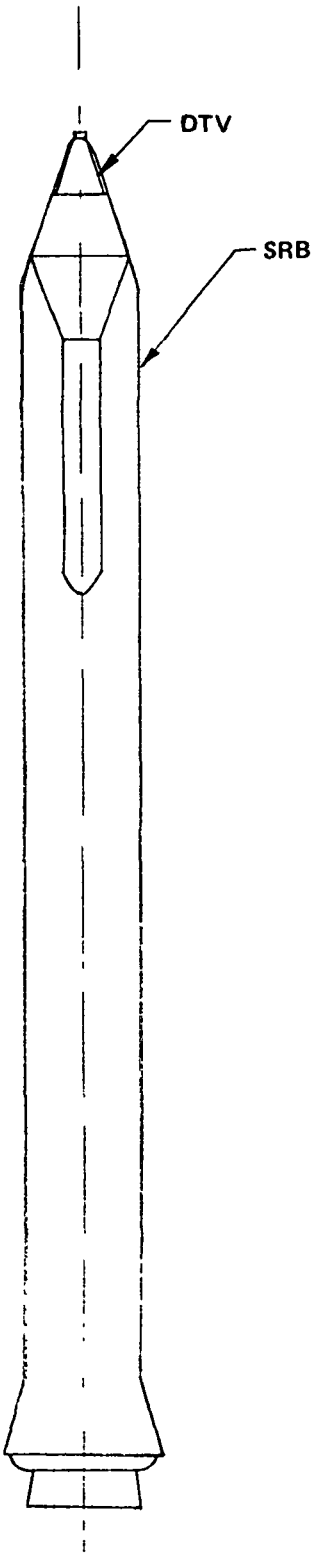

Figure 2-3. THE DTV AND THE SRB OUTLINES

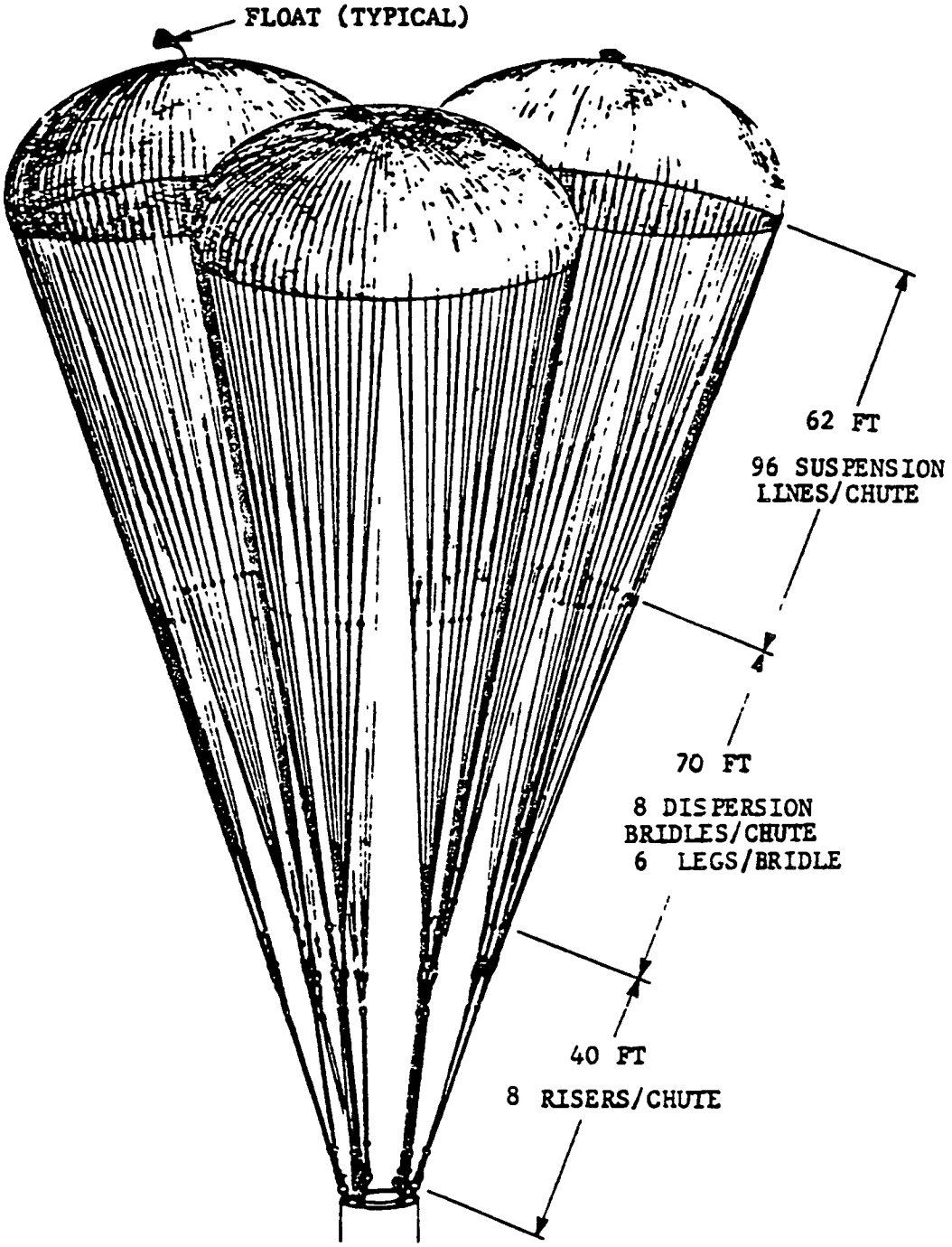

Figure 2-4. MAIN PARACHUTE GEOMETRY

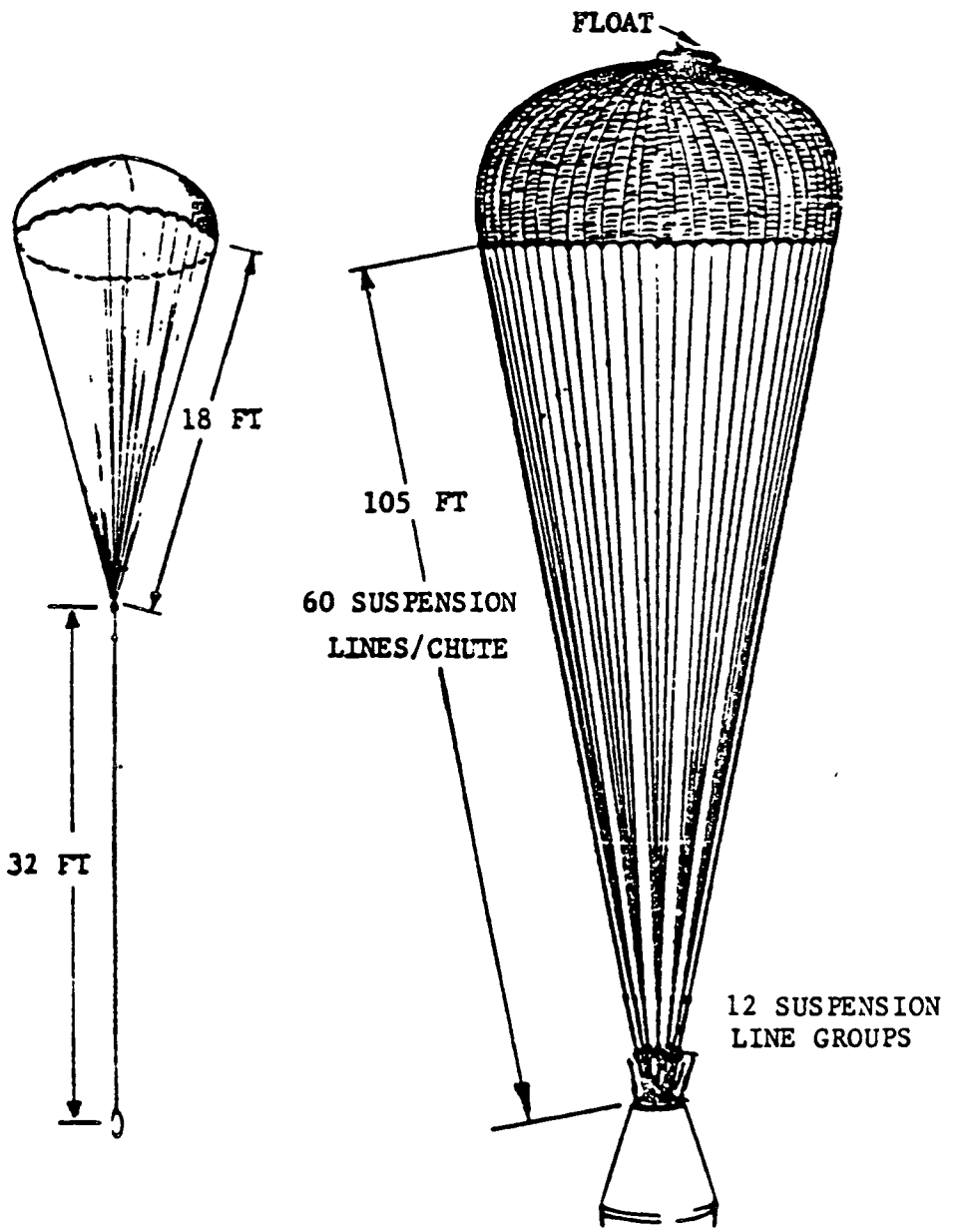

Figure 2-5. DROGUE AND PILOT PARACHUTE GEOMETRY

Section III

SRB REENTRY FLIGHT AND DTV DROP TEST ENVIRONMENTS

The SRB recovery sequence begins at an altitude near 4.7 km and dynamic pressure of about 9,576 N/m^2 when the nose cap is ejected by firing nose cap thrusters. The nose cap deploys a pilot chute which at inflation deploys a drogue chute. In this deployment environment the SRB is in a broadside attitude and descending with high attitude rates. The drogue chute attains a reefed inflation and orients the SRB to a near tail first attitude. After inflation to a second reefed stage the drogue chute separates the frustum from the SRB while deploying the main chute cluster in their first reefed stage. The main chutes subsequently inflate to a second reef stage, and to a full open configuration, and produce sufficient drag force to decelerate the SRB to a water impact velocity of about 26m per second. The dynamic pressure history for the SRB nominal descent case is presented in Figure 3-1.

In the case of the air drop tests, the sequence of operations begins when a drogue gun fires a 0.45kg slug with a certain velocity to pull off the vane parachute. The vane parachute deploys the nose cap cover followed by the nose cap extraction and the pilot chute. Contrary to the SRB case, the nominal DTV attitude at this time is near zero degrees angle-of-attack. However, in DAD's 1 and 2, because of a DTV instability, the DTV angles-of-attack at nose cap deployment were about 70-degrees and 36-degrees respectively. The DTV attitudes in the DAD's 2, 4, 5, and 6 being different from the SRB case, the drogue chute deployment dynamics observed in these air drops is not representative of the prototype case.

The DAD's were performed to achieve specific objectives. Table 3-1 summarizes the specific objectives of each air drop test including the parachutes tested. Table 3-2 presents pertinent data from each drop test. Since the drop test vehicle is only about one-third the weight of the SRB, the target test conditions, dynamic pressure and altitude, were matched at one point in a particular drop test to meet the specific test objective. Also, the reefing line lengths and the reefing cutter times used as shown in Table 3-2 do not

necessarily represent their flight values and were used to achieve target conditions. Table 3-3 presents target test conditions in each DAD at which they matched particular conditions on the SRB. Figure 3-1 shows that at line stretch both the drogue chute and the main chute(s) encompassed the flight nominal dynamic pressure.

As an aid to the analysis of DAD's data a brief discussion of each test is given below:

DAD-1

The objective of the DAD-1 was to deploy the DSS drogue parachute in the dynamic pressure and altitude environment associated with the SRB DSS limit load condition at the first reefed stage. The objective was not achieved. This resulted from the instability of the DTV after drop when it underwent coning motion with a total angle-of-attack of up to 70-degrees. The terminal space-position data for the full open drogue chute was not available because only the DTV was followed after frustum separation.

DAD-2

The objective of the DAD-2 was to deploy a single main parachute in the dynamic pressure environment associated with SRB main chute limit load at first reefed stage. The objective was achieved and the single main parachute was subjected to an overload condition of 15.4 percent above its design limit load at first reef stage. The DTV exhibited instability similar to that observed in air drop test 1. The terminal space-position data for the full open drogue chute was not available.

DAD-3

The objective of the DAD-3 was to deploy the drogue chute in a dynamic pressure environment associated with a first reefed stage overload condition. This test failed resulting in major damage to the drogue parachute, the main parachutes and the DTV. This was due to the failure of the drogue chute first stage reefing line retention band, and an overload condition for the second stage reefing line and the vent band. Beginning with this test, three fins were added to the DTV for stability.

DAD-4

The objective of the DAD-4 was to deploy the DSS main parachute cluster in a high dynamic pressure environment. The test was successful in achieving 36 percent overload condition at the main chutes line stretch. The DTV was stable and had a roll rate of about 18 degrees per second prior to frustum separation. No space-position data was available for the drogue chute second reef stage.

DAD-5

The objective of the DAD-5 was to deploy the DSS drogue chute in a dynamic pressure environment associated with a first reefed stage overload condition. The drogue chute was subjected to a peak load of 12.9 percent above the design limit load, and the test was successful. The accelerometers response data was not available for the main parachutes because of telemetry cut-off at frustum separation. Space position data, however, was available. During flight the drogue chute frustum combination overtook the main chutes cluster. In so doing, the frustum tore and went thru one main chute which finally collapsed. The DTV continued to descend under the remaining two main chutes.

DAD-6

The objective of the DAD-6 was to test a single main chute to a total load at least as high as its maximum expected operating load. This load condition was achieved by going directly to the second reefed stage on the single main chute. The main chute was subjected to 15.4 percent overload above the design limit load, and the drogue chute was subjected to maximum expected SRB environment. The test was successful. Both the telemetry and the space-position data was available for required events.

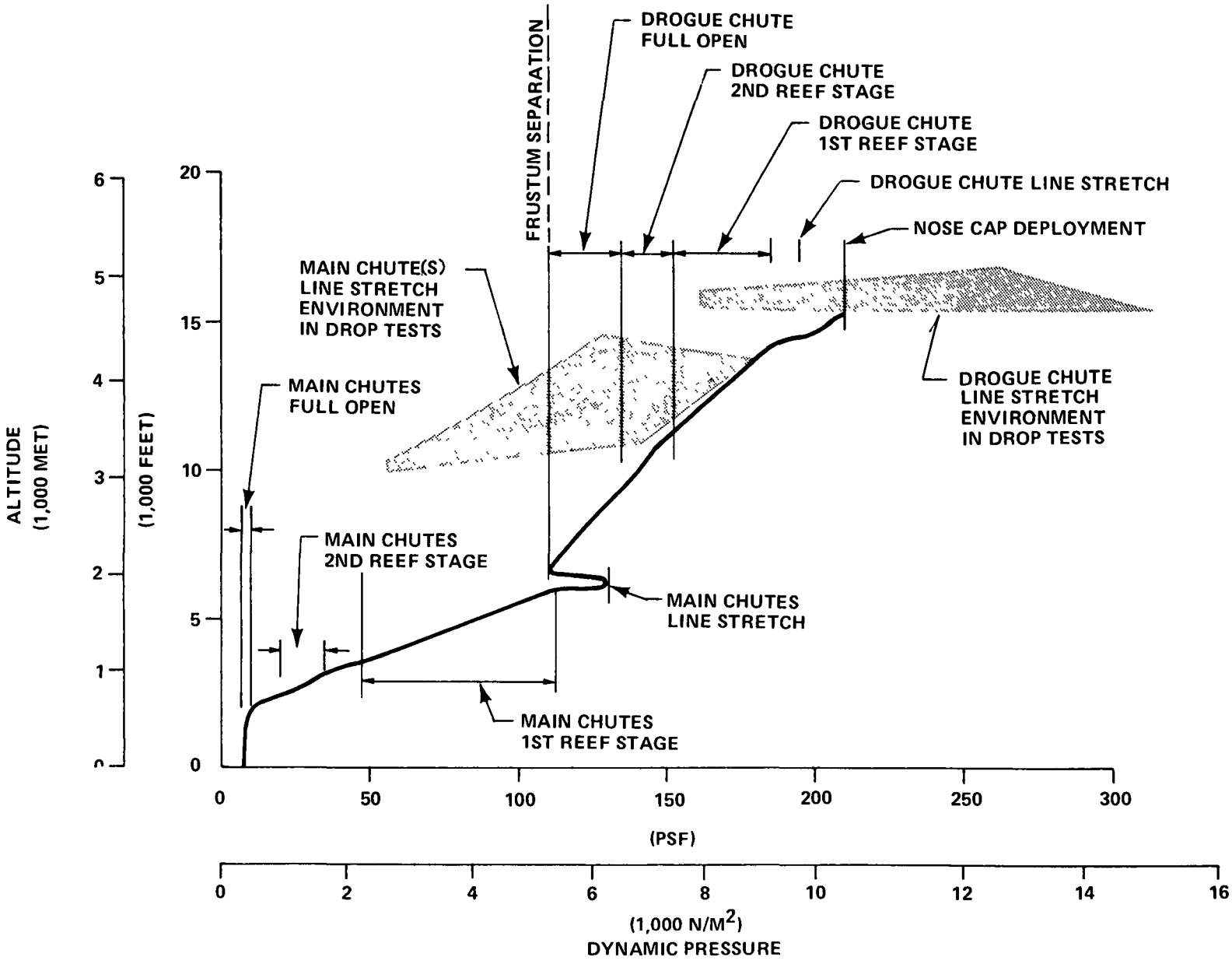

Figure 3-1. DSS DYNAMIC PRESSURE HISTORY FOR NOMINAL DESCENT

Table 3-1. AIR DROP TEST OBJECTIVES

DROP TEST NO.	PARACHUTES	OBJECTIVE
1	Drogue, Main Chute Cluster	SRB drogue chute limit load condition at the first reef stage.
2	Drogue, Single Main	SRB main chute limit load condition at the first reef stage.
* 3	Drogue, Main Chute Cluster	SRB drogue chute over load condition at the first reef stage.
4	Drogue, Main Chute Cluster	SRB main chute cluster deployment in high q environment.
5	Drogue, Main Chute Cluster	Repeat of Drop Test 3.
6	Drogue, Single Main	SRB main chute load at least as high as its maximum expected operating load.

**Test unsuccessful, no useful data obtained*

Table 3-2. AIR DROP TESTS SUMMARY

DROP TEST NUMBER	REEFING LINE LENGTHS, L_R/D_o		REEFING CUTTER TIMES (sec)		q_∞ AT LINE STRETCH (N/m^2)		WEIGHT ON (kg)	
	DROGUE	MAIN(S)	DROGUE	MAIN(S)	DROGUE	MAIN(S)	DROGUE	MAIN(S)
1	1.6, 1.9	0.492, 0.834	7, 12	10, 17	8,140	2,653	21,541	18,955
2	0.68	0.492, 0.834	7, 12	10, 17	7.809	6,756	21,757 3,896†	17,810
3*	1.36,1.80	0.54, 1.08	7, 12	10, 17	-	-	-	-
4	1.15, 1.48	0.54, 1.08	6, 10	10, 17	14,288	8,580	21,664 2,546†	19,092
5	1.36, 1.80	0.54, 1.08	7, 12	10, 17	15,197	2,662	21,664	19,092
6	1.36	1.08	10	10	12,593	6,148	21,255 3,665†	17,591

**Test unsuccessful, no useful data obtained.*

†*Weight on drogue chute beginning second reef stage.*

Table 3-3. AIR DROP TEST CONDITIONS

AIR DROP NO.	EVENT	ALTITUDE (m)			DYNAMIC PRESSURE (N/m^2)			REMARKS
		TARGET	DROP TEST	FLIGHT NOMINAL	TARGET	DROP TEST	FLIGHT NOMINAL	
1.	Drogue chute inflation at 1st reef	-	4,671	4,353	10,342	7,915	8,906	Drogue chute limit load not achieved.
2.	Frustum separation	-	-	2,011	5,722	5,468	5,315	Main chute limit load at 1st reef stage achieved.
	Main chute inflation at 1st reef	-	3,176	1,762	-	5,425	5,554	
3.	Drogue chute inflation at 1st reef	-	4,356	4,353	-	14,517	8,906	Drogue chute failed after inflation. Main chute failed.
	Nose cap separation	4,668	4,676	4,922	13,464	14,517	10,055	
4.	Frustum separation	4,358	4,289	2,011	7,278	8,092	5,315	Overload at main chutes line stretch achieved.
	Main chute inflation at 1st reef	-	3,952	1,762	-	5,425	5,554	
5.	Nose cap separation	5,001	4,922	4,685	13,641	14,158	10,055	Drogue chute overload condition achieved.
6.	Frustum separation	4,706	4,614	2,011	4,620	5,171	5,315	Drogue chute subjected to maximum expected SRB environment. Main chute subjected to overload at 2nd reef stage.

Section IV

DROP TEST ANALYSIS

The results of the Development Air Drop Tests performance analysis are presented in this section. Three different aspects of parachute performance are discussed: parachute drag performance, parachute filling times, and parachute deployment dynamics. The data used to calculate parachute performance was wind-corrected space-position data, and filtered accelerometer responses. The motion picture films were used to determine parachute filling times, parachute deployment dynamics, and observe parachute stability.

4.1 TERMINAL DRAG PERFORMANCE

Under terminal conditions a body reaches a terminal velocity as a result of an equilibrium between the body weight and the drag. The terminal drag performance of the DSS parachutes was calculated using the following relationship:

$$C_D S = \frac{W}{\frac{1}{2} \rho V_z V_T} - (C_D S)_v \qquad (4\text{-}1)$$

Here

W = Total system weight (kg)

ρ = Air density (kg/m^3)

V_z = Vertical component of velocity (m/sec)

V_T = Total velocity (m/sec)

$(C_D S)_v$ = Drag area of the DTV or frustum (m^2)

The values of velocities used in equation (4-1) were obtained from the space-position data. The full open drag areas of the parachutes were calculated over a time interval about 2 seconds prior to DTV/frustum impact. The terminal drag coefficients were then obtained by dividing averaged drag areas calculated using equation (4-1) by the parachutes reference areas. The values of the terminal drag coefficients thus calculated are tabulated in Table 4-1 and are plotted as a function of the canopy loading, $W/C_D S$ in Figure 4-1. The Arabic numerals with the symbols refer to various DAD's. The drag coefficient value for the drogue chute in the DAD-1 was taken from reference 8 since the terminal velocity components for this test were not available from

the space-position data. Also, the terminal velocity components in DAD-5 were taken before the drogue chute/frustum combination overtook the main chutes cluster which eventually resulted in the failure of one of the main chutes.

Table 4-1. TERMINAL DRAG PERFORMANCE OF THE DSS PARACHUTES

AIR DROP NO.	DRAG AREA C_DS (m^2)	DRAG COEFFICIENT C_D
DROGUE PARACHUTE		
1	132.9	0.620
2	-	-
4	109.3	0.504
5	136.8	0.595
6	146.1	0.639
SINGLE MAIN PARACHUTE		
2	600.7	0.619
6	622.4	0.636
MAIN CHUTES CLUSTER		
1	1,725	0.595
4	1,809	0.700
5	1,675	0.577

The terminal drag coefficient values presented in Figure 4-1 include forebody interference effects, and any space position data error in the values of velocities. The drag coefficient values for the DAD-4 are observed to be either abnormally low for the drogue chute or abnormally high for the main chute cluster. The DAD-4 drag coefficient values will therefore be discarded while averaging out DAD data to determine nominal values of the drag coefficient. The interference free values of the drogue chute drag coefficient calculated from the earlier wind tunnel test data (References 1 and 3) are also shown in Figure 4-1. The DAD values of the drogue chute drag coefficient, with interference effects, are generally lower than the wind tunnel data.

The DSS parachutes drag performance estimates were made in reference 4. Figures 4-2 through 4-4 are reproduced from reference 4 and present the interference free drag coefficient for the DSS parachutes and the interference effects behind an SRB forebody. Based on this study the full open drag coefficient for the SRB drogue chute (for an effective L_s/D_o = 2.1, and a trailing distance, x/D_o = 1.96) and the main chute cluster (for an effective L_s/D_o = 1.3) were estimated to be 0.65 and 0.62 respectively. The DAD values for the terminal drag coefficients of the DSS parachutes along with their predicted values are replotted in Figure 4-5. The average value for the drogue chute drag coefficient is 0.619 which is about 5 percent less than that predicted in reference 4. From the limited drop tests data on the main chute(s) in Figure 4-5, it is apparent that there is some degradation in drag due to cluster interference. The single main chute drag coefficient is 0.628 compared to 0.62 predicted in reference 4. The average drag coefficient for the main chute cluster is 0.586 showing about 7 percent drag loss due to cluster interference.

4.2 REEFED DRAG PERFORMANCE

The reefed drag performance of the DSS parachutes was calculated using the following equations:

$$C_D S = \frac{-W}{q}\left(\frac{V_z}{V_T} + \frac{a_T}{g}\right) - (C_D S)_v \qquad (4\text{-}2)$$

$$C_D S = \frac{nW}{q} - (C_D S)_v \qquad (4\text{-}3)$$

Here
- C_D = Drag coefficient of the parachute
- S = Parachute reference area (m^2)
- n = Total vehicle acceleration (no. of g's)
- W = Total system weight (kg)
- q = Dynamic pressure (N/m^2)
- V_z = Vertical component of velocity (m/sec)
- V_T = Total velocity (m/sec)
- a_T = Tangential acceleration (m/sec^2)
- g = Gravitational acceleration (9.81 m/sec^2)
- $(C_D S)_v$ = Drag area of the DTV or frustum (m^2)

The values of velocities, tangential acceleration, and dynamic pressure used in equation (4-2) were obtained from the space-position data. There is a large variation in the values of tangential acceleration, a_T, computed as the second derivative of the space-position data. The filtered accelerometer response data used in equation (4-3) is less noisy. Therefore, equation (4-3) was used, whenever possible, to determine the reefed parachute performance. Sufficient time was allowed after inflation at any stage to allow the initial overload oscillations to damp out before calculating the drag areas. The average steady state drag areas obtained using the above equations were divided by the parachute reference area to determine the drag coefficients. The values of reefed drag coefficients are tabulated in Table 4-2 and are plotted against the nondimensional reefing line length, L_R/D_o in Figure 4-6. The Arabic numerals with the symbols refer to the DAD numbers. It is observed that most of the single chute (drogue chute, and single main chute) data fits on the same straight line. The maximum variation in the values of the reefed drag coefficients is about 13 percent.

The single chute reefed drag coefficient data fit curve is replotted with the wind tunnel test data (Ref. 3) in Figure 4-7. It compares well with the wind tunnel test results in that the reefed drag coefficients of both the drogue parachute and the single main parachute are approximated by the same linear function of the nondimensional reefing line length. However, the wind tunnel tests indicate lower drag coefficients and the results seem to be displaced by a constant value. It was noted in reference 3 that the reefed drag coefficients obtained in the wind tunnel tests were lower than expected because of stiffer models. In an effort to predict the reefed drag performance (Ref. 4) of the DSS parachutes the available data was gathered on 20-degree conical ribbon parachutes and a curve was selected for the DSS parachutes. Figure 4-8 reproduced from reference 4 shows the predicted curve for the reefed DSS parachutes, and fits exactly on the reefed drag performance calculated using the drop test data.

It is observed from Figure 4-6 that the reefed main chute cluster drag coefficients are higher than the single chute drag coefficients. A similar observation on the reefed drag coefficients was made from the wind tunnel test results (Ref. 3). The reefed main chute cluster drop test drag data

is replotted with the wind tunnel test data (Ref. 3) in Figure 4-9. Again, the wind tunnel test values of the reefed drag coefficient are lower than the drop test values and seem to be displaced by a constant value. Figure 4-10 presents plots of the reefed cluster efficiency obtained from the drop tests and the wind tunnel tests. In the wind tunnel tests, the cluster efficiency was observed to increase almost linearly with the reefing line length. In the drop tests, the increase in the cluster efficiency continues up to a reefing line length ratio, L_R/D_o of 1.0, and then exhibits a decreasing trend at higher values of the reefing line length.

Table 4-2. REEFED DRAG PERFORMANCE OF THE DSS PARACHUTES

AIR DROP NO.	REEFING LINE LENGTH, L_R/D_o	DRAG AREA C_DS (m^2)	DRAG COEFFICIENT C_D
DROGUE PARACHUTE			
1	1.6	89.2	0.419
1	1.9	106.6	0.501
2	0.68	35.6	0.167
4	1.15	65.0	0.306
5	1.364	76.0	0.357
5	1.8	107.0	0.503
6	1.364	71.9	0.338
SINGLE MAIN PARACHUTE			
2	0.492	87.3	0.091
2	0.834	174.6	0.181
6	1.08	256.8	0.266
MAIN CHUTES CLUSTER			
1	0.492	288.1	0.099
1	0.834	577.2	0.199
4	0.54	343.5	0.119
4	1.08	935.6	0.323
5	0.54	313.4	0.108
	1.08	869.8	0.300

4.3 PARACHUTE FILLING TIMES

The parachute filling time were determined using the timeline of the parachute deployment sequence for each drop test. Table 4-3 presents the filling times for the drogue parachute and the single main parachute. The filling times for the main chute cluster have not been included to exclude any cluster interference and blanketing effects while comparing single parachute results. The filling times for the first reefed stage were obtained by subtracting the time at bag strip from the time at parachute inflation for the first reefed stage. The filling times for the other reefed stages were obtained by subtracting the time at disreef for the previous stage from the time at inflation for the particular stage. Figure 4-11 presents the filling times for various reefing line lengths. The Arabic numerals with the symbols refer to the DAD numbers. A reefing line length of 2.1 times the nominal diameter was assumed for the full open parachute. The data points in Figure 4-11 do not take into account the velocity at which the parachute was inflated to a particular stage. In addition, they do not reflect the reefing stage at the beginning of inflation. Thus, the filling times as plotted in the Figure 4-11 provide no valuable information. In Figure 4-12 the parachute filling times are presented as a function of the velocity at the start of inflation. The numerical values with the symbols refer to the difference in the parachute mouth diameter at the beginning and the end of inflation. Again, the filling time data as plotted in Figure 4-12 does not provide any definite trends to predict the parachute filling times.

Analytically, the parachute filling times have been determined using a general equation of the type:

$$t_f = \frac{K\ D}{V_{BS}} \tag{4-4}$$

where, D is a characteristic diameter, V_{BS} is the velocity at the start of the inflation process, and K is a nondimensional filling time. Several theories have been put forward as to the form of characteristic diameter for the reefed stages, eg, the difference between the square roots of the final and the initial drag areas $(\psi_2^{\frac{1}{2}} - \psi_1^{\frac{1}{2}})$, the difference between the final and the initial projected diameters, etc. In this analysis, D has been taken to be the difference between the final and the initial reefed diameters. There

have been arguments against using the reefing diameter as a characteristic length because it has no well defined relationship with the volume of the inflated portion of the canopy. However, because of the simplicity in its calculation and knowledge that the filling times are going to be predicted based on empirical data for a system, the reefing diameter has been chosen as the characteristic length in the filling time equation.

The nondimensional filling time, K, depends upon the reefed dimensions and the velocity - the two quantities basically affecting the filling time for a reefed stage, and is thus a good reference to predict the filling times for actual flight conditions.

$$K = \frac{t_f \, V_{BS}}{\Delta D} \tag{4-5}$$

Here, t_f is the measured filling time. The velocity term, V_{BS}, for the first reef stage is taken to be the velocity at bag strip, while for subsequent stages it represents the velocity at the start of inflation for that stage. The reference dimension, ΔD, is the difference between the reefed diameters at the end and the start of inflation process. For the first reefed stage, the parachute pack diameter at the base is considered to be the reefed diameter at the start of inflation, and for the full open case, the reefed diameter at the end of inflation is calculated by considering full open skirt circumference to be 2.1 times the parachute nominal diameter.

The nondimensional filling time, K, is plotted as a function of the reefing line length ratio, L_R/D_o, in Figure 4-13. It is observed from the figure that most of the data for the reefed chutes and the full open main chute follows a general trend. However, a large variation from this general trend is observed for some cases, especially for the full open drogue chute in DAD's 1 and 5, and the first reefed stage in DAD-2. The high values of K in the full open case can be due to errors in measuring precisely the time for full inflation. The nondimensional filling time curve thus obtained can be utilized to predict the filling times for the SRB parachutes. Detailed correlations can be made for each reefed stage and the filling times by studying the area growth curves for each stage. However, no attempt is being

made here to attempt the correlations and thereby assess tolerance levels on the K values.

Table 4-3. PARACHUTE FILLING TIMES

AIR DROP NUMBER	REEFING LINE LENGTH, L_R/D_o	VELOCITY AT START OF INFLATION, V_{BS} (m/sec)	FILLING TIME t_f (sec)
DROGUE CHUTE			
1	1.6	149	0.53
	1.9	86	0.09
	F.O.	73	0.2
2	0.68	145	1.05
4	1.15	194	0.571
5	1.364	204	0.65
	1.8	102	0.115
	F.O.	79	0.15
6	1.364	194	0.613
SINGLE MAIN CHUTE			
2	0.492	126	1.57
	0.834	69	1.84
	F.O.	45	1.51
6	1.08	131	2.065
	F.O.	44	1.18

It is relevant here to discuss the opening characteristics of the parachutes as observed in the various DAD's. As a general trend the main parachutes were slow to reach their steady state areas at any stage of inflation. This was particularly noticed in the case of the main chute first reefed stage in DAD-2. In DAD-6 the main chute did not appear to have acquired a fully developed configuration in its reefed stage. This condition persisted even in the full open configuration and the canopy had a caved in planform. The canopy area growth curves of the DSS parachutes were obtained from the onboard cameras. The parachutes projected areas were measured and were normalized by the respective full open projected areas. Figures 4-14 through 4-22 depict area ratios for the typical cases and are reproduced from references 8 and 9.

The main chute cluster inflation in the DAD numbers 1, 4, and 5 was observed to be uniform. There was simultaneous extraction of all the chutes in the cluster and there was no evidence of the two lead parachutes blanketing out the third lag parachute. However, the parachute filling times for their first reefed stage were measured to be different for different chutes in the cluster. Also, there was evidence of non-synchronous firing of reefing line cutters which resulted in general non-synchronous opening in the second reef stages and full open conditions.

4.4 PARACHUTE DEPLOYMENT DYNAMICS

The success of a recovery program depends on an orderly deployment of its parachutes. Every deployment method, selected for a specific mission, being different there are no hard and fast rules to improve on its performance. However, there are guidelines which are incorporated in general design procedures for a satisfactory deployment. Generally, the deployment of a parachute depends upon the way the canopy is folded and packed inside the bag. The deployment dynamics of a parachute is a function of the canopy restraints and the weight to drag ratio of the deploying parachute or a system. A high weight to drag ratio of the deploying parachute may result in a 'Line Sail' of the deploying parachute or an 'Inflation Overtake' of the parachute being deployed. Excessive extraction forces (low weight to drag ratio of the deploying system) on the other hand can result in damage to the parachutes because of canopy restraints.

Generally, the deployment of the DAD parachutes and the canopy strip-outs were observed to be orderly. In DAD-2 the drogue chute lines exited the bag as if being dumped out showing low bag strip velocity. This also resulted in an inflation overtake of the main chute in which the canopy inflated faster than the rate at which it was being pulled. The drogue chute drag to weight ratio in this case was measured to be 0.05 which is lower than an estimated critical value of 0.1 (Ref. 8) to avoid line sail or inflation overtake. Efforts were made to increase the drag to weight ratio of the drogue chute in the remaining air drop tests which did not experience any line sail.

Some comments need to be added here on the DSS parachutes stability. Invariably in all the tests the pilot chute was observed to breathe, a phenomenon which is generally associated with small parachutes tested in wind tunnels. A similar observation was made in the DAD-2 in which the reefed drogue chute breathed. Also, in DAD-5 the full open drogue chute suspension lines before frustum separation underwent lateral oscillations and the lines appeared to have slack. This line whipping diminished in magnitude after frustum separation when the drogue chute was attached to the frustum only. These comments are reported as general observations. No attempt is made to establish the conditions for parachute stability.

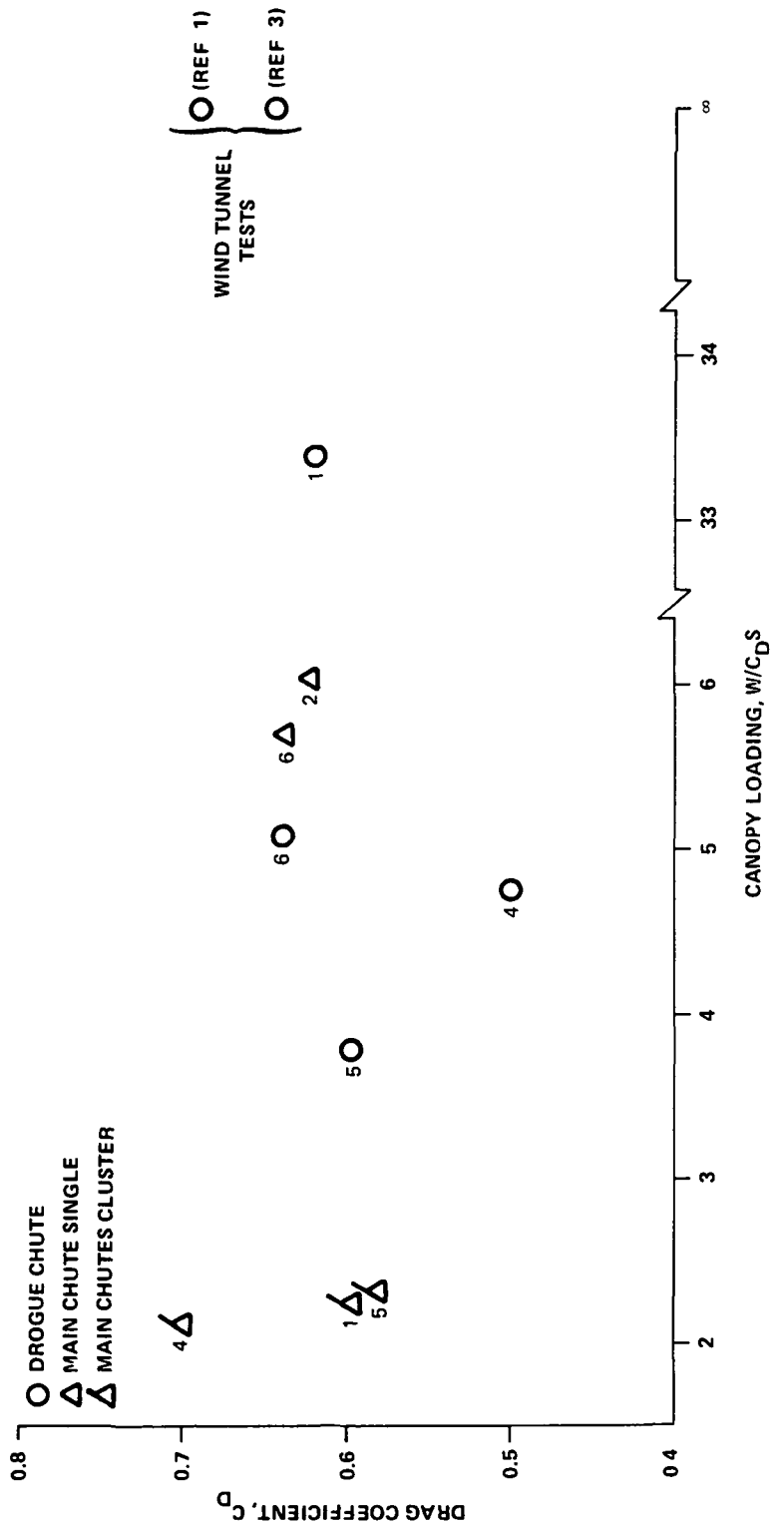

Figure 4-1. TERMINAL DRAG COEFFICIENT OF THE DSS PARACHUTES

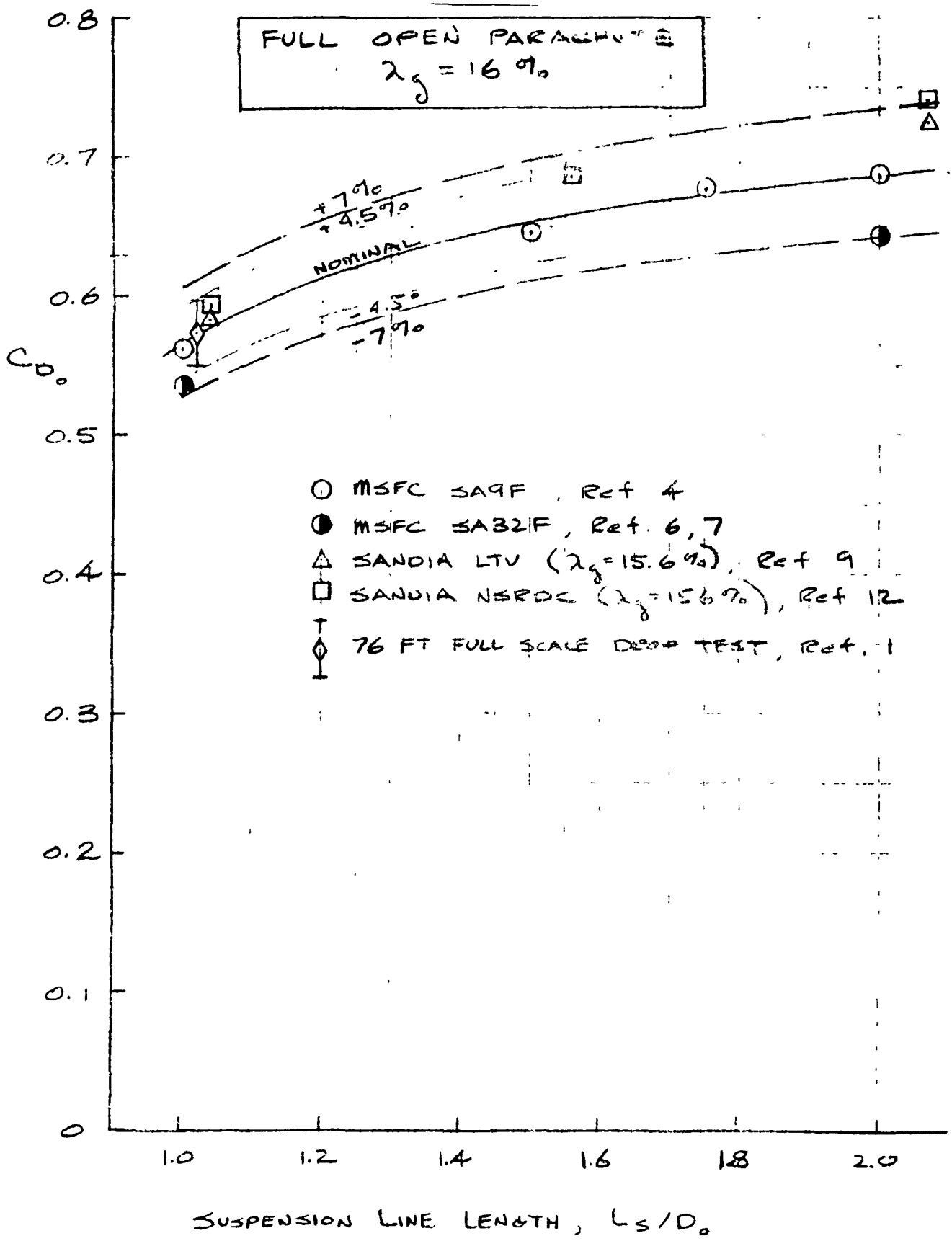

Figure 4-2. INTERFERENCE FREE DRAG PERFORMANCE OF 20-DEGREE CONICAL RIBBON PARACHUTES.

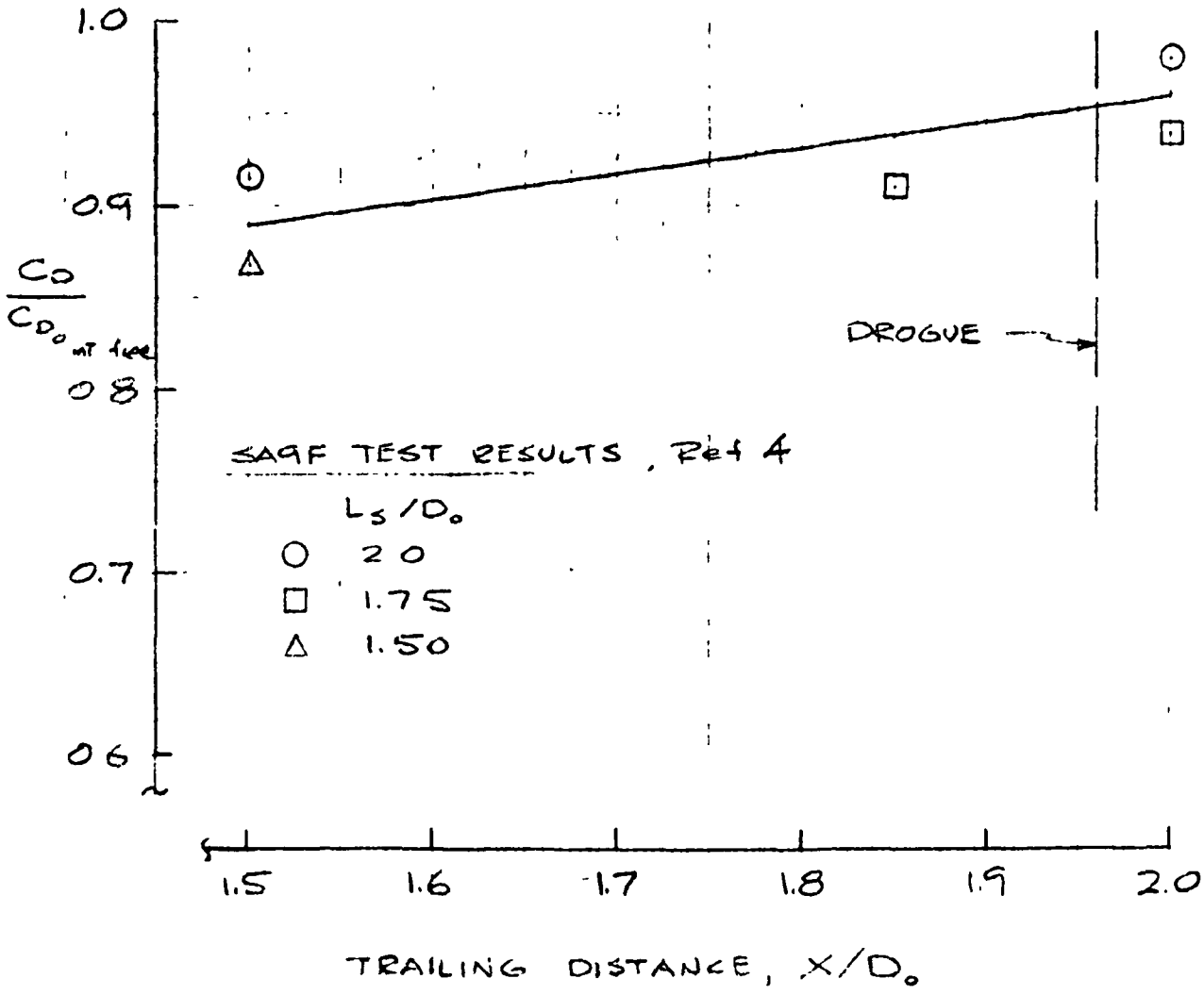

Figure 4-3. DROGUE PARACHUTE DRAG LOSS DUE TO FOREBODY INTERFERENCE

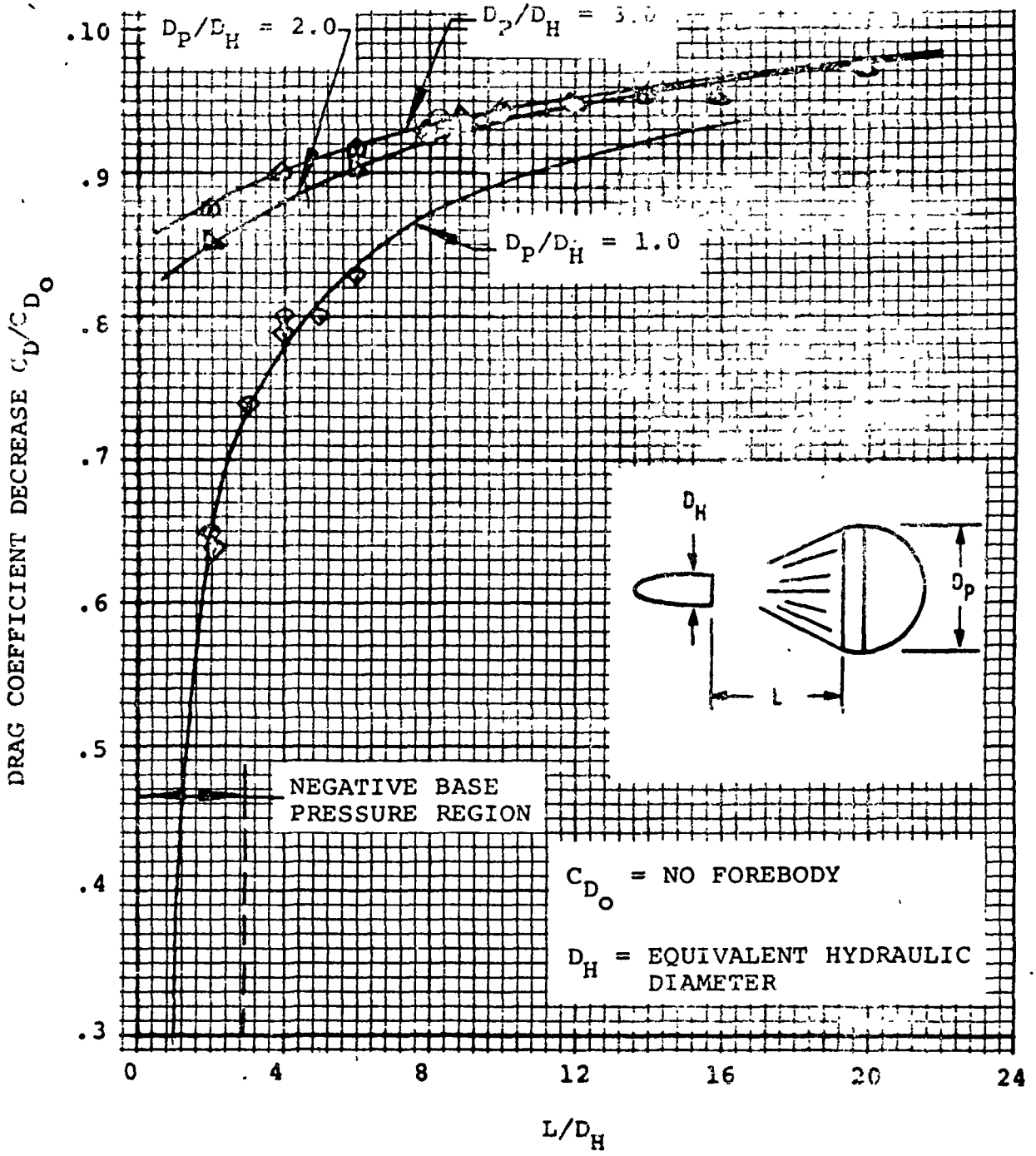

Figure 4-4. PARACHUTE DRAG LOSS AS A FUNCTION OF TRAILING DISTANCE AND FOREBODY DIAMETER

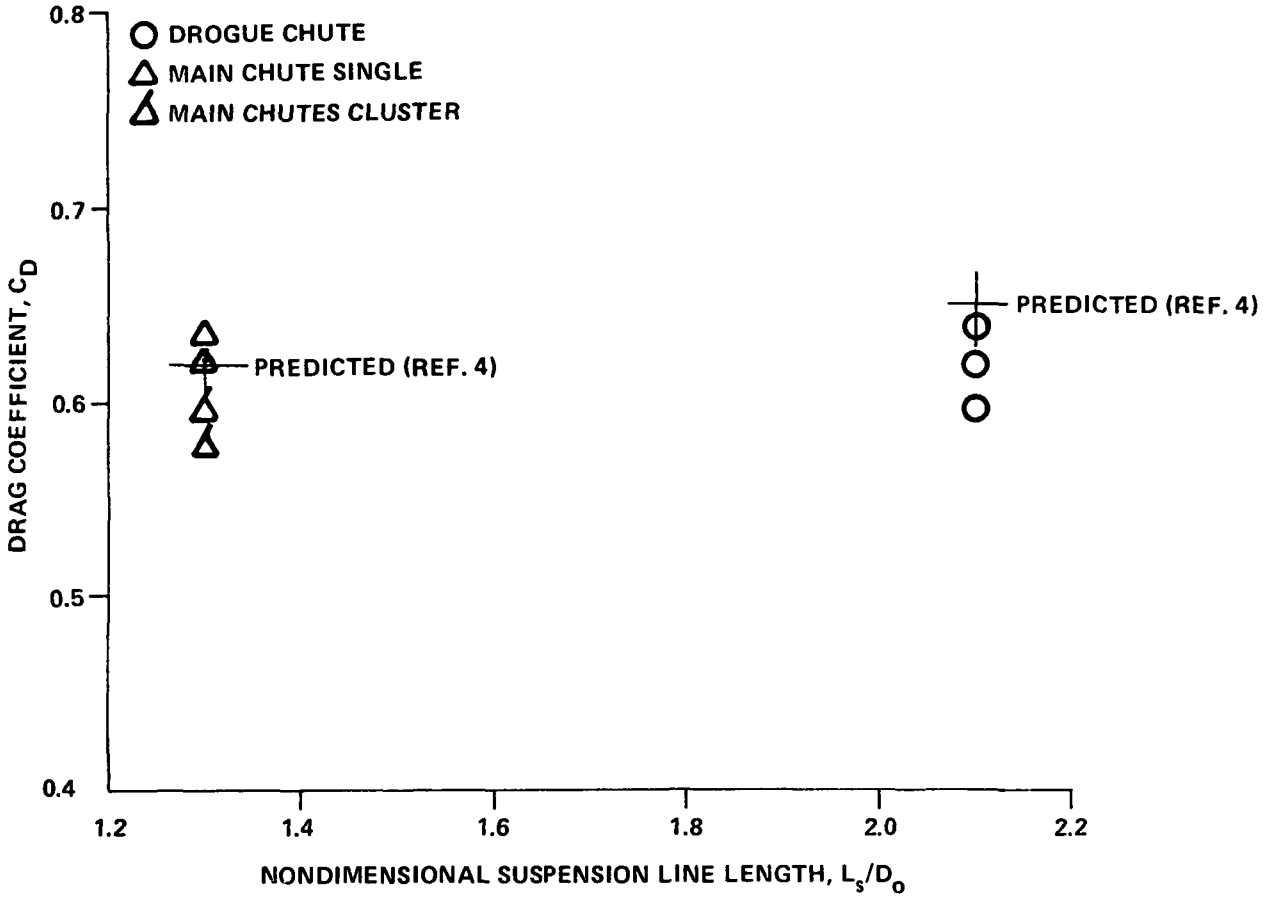

Figure 4-5. COMPARISON OF DROP TEST WITH PREDICTED DSS PARACHUTES DRAG COEFFICIENT

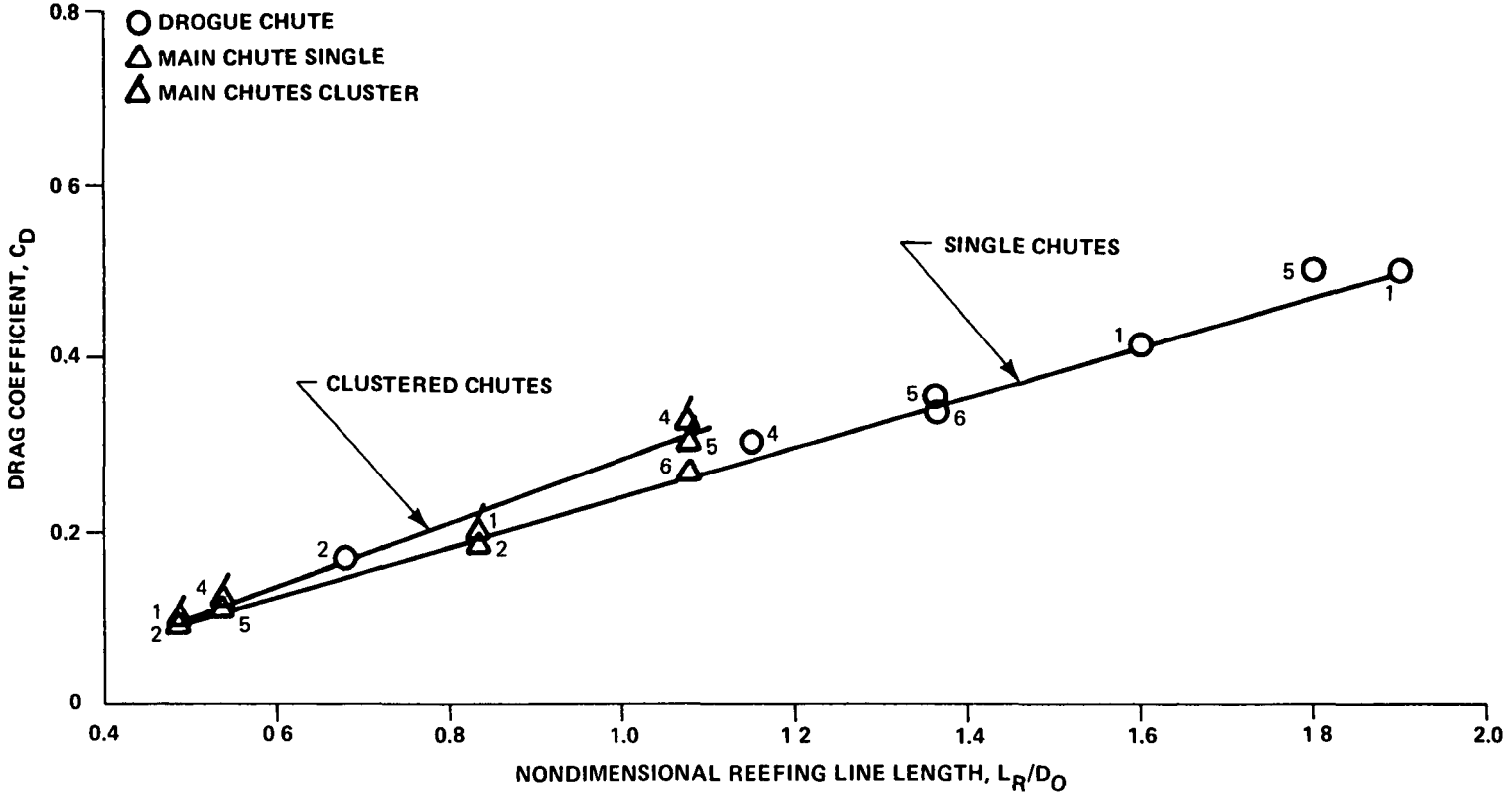

Figure 4-6. REEFED DRAG COEFFICIENT OF THE DSS PARACHUTES

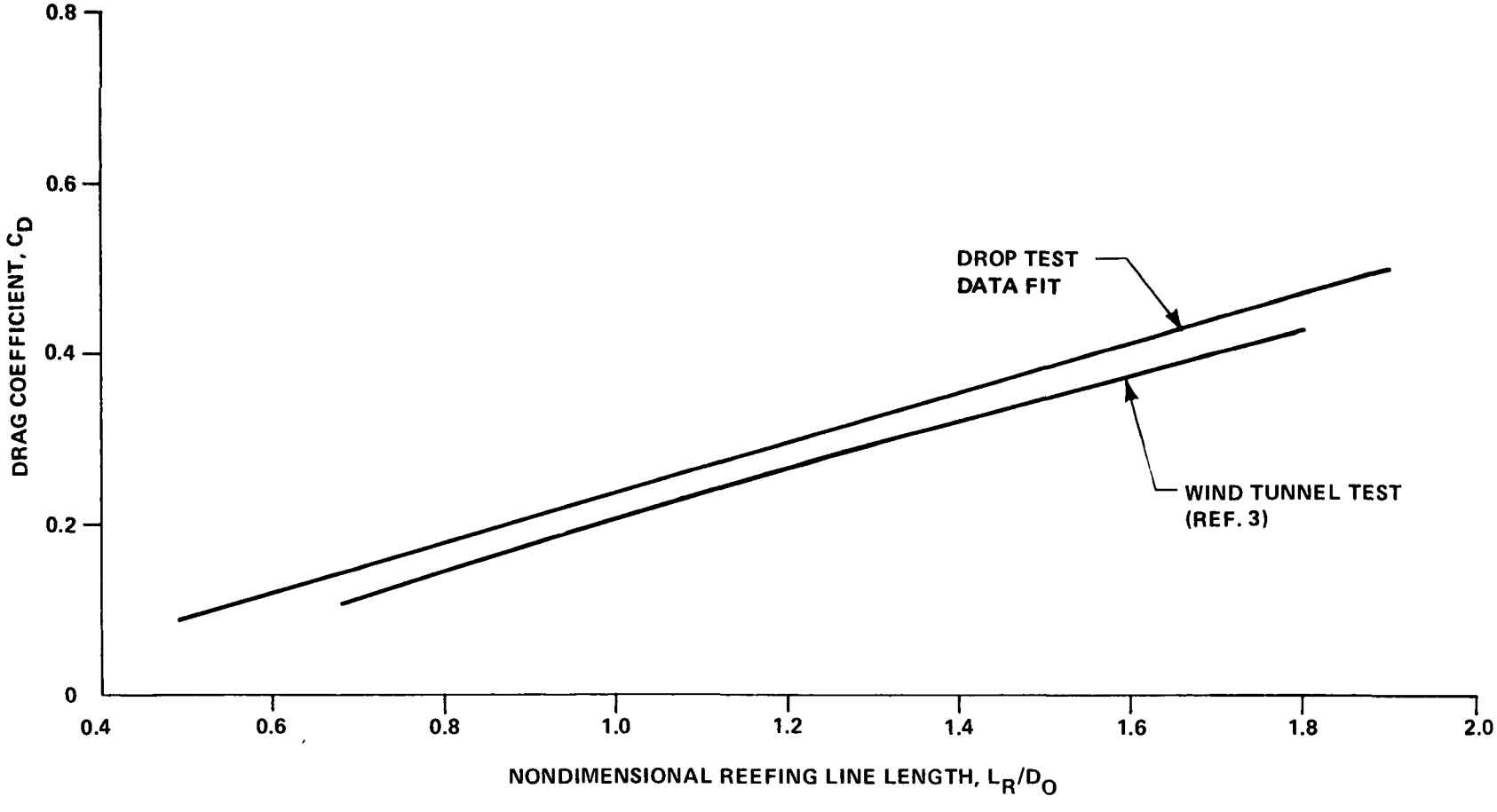

Figure 4-7. SINGLE CHUTE REEFED DRAG COEFFICIENT

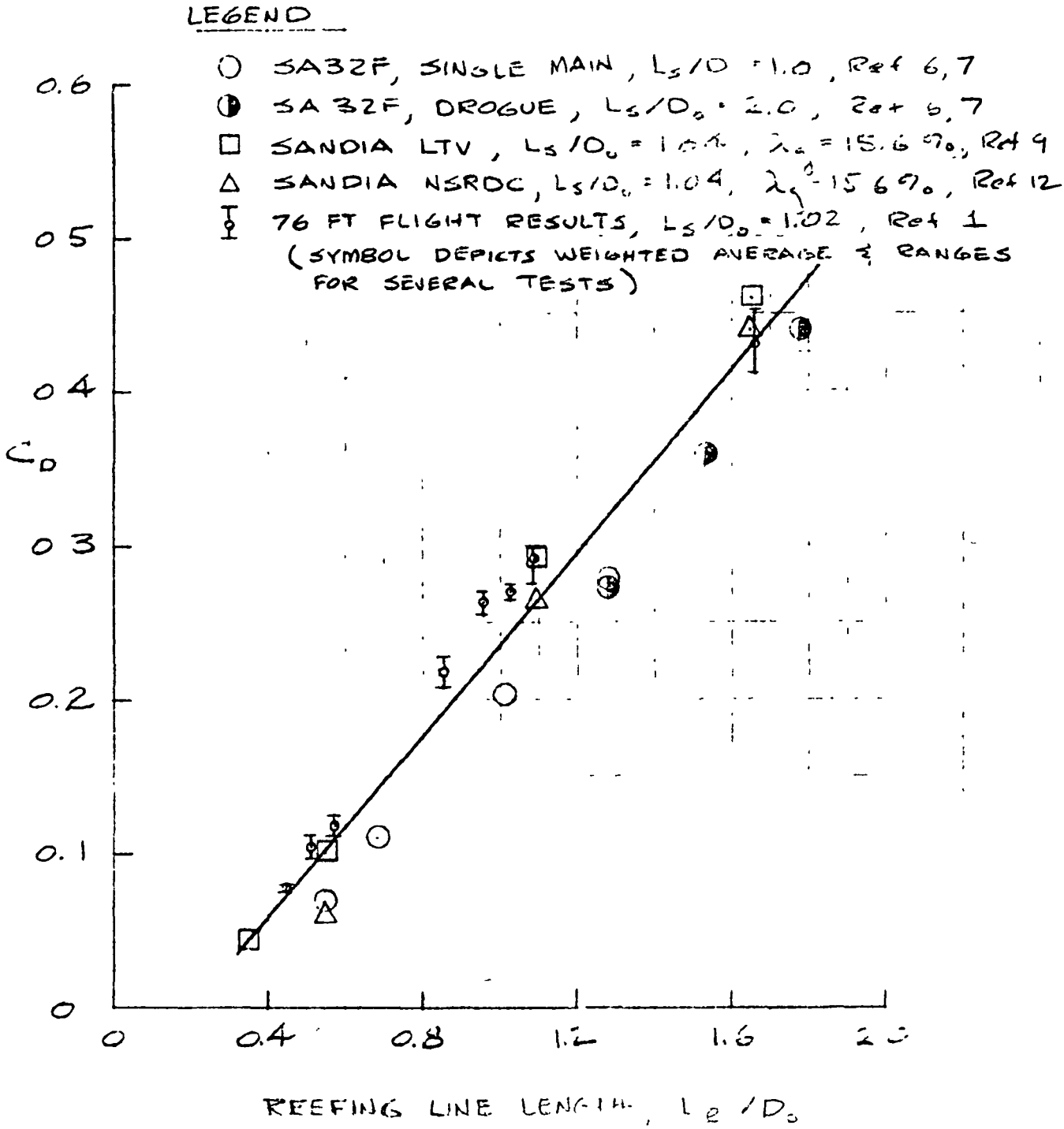

Figure 4-8. EFFECT OF REEFING ON INTERFERENCE FREE DRAG CHARACTERISTICS OF 20-DEGREE CONICAL RIBBON PARACHUTE

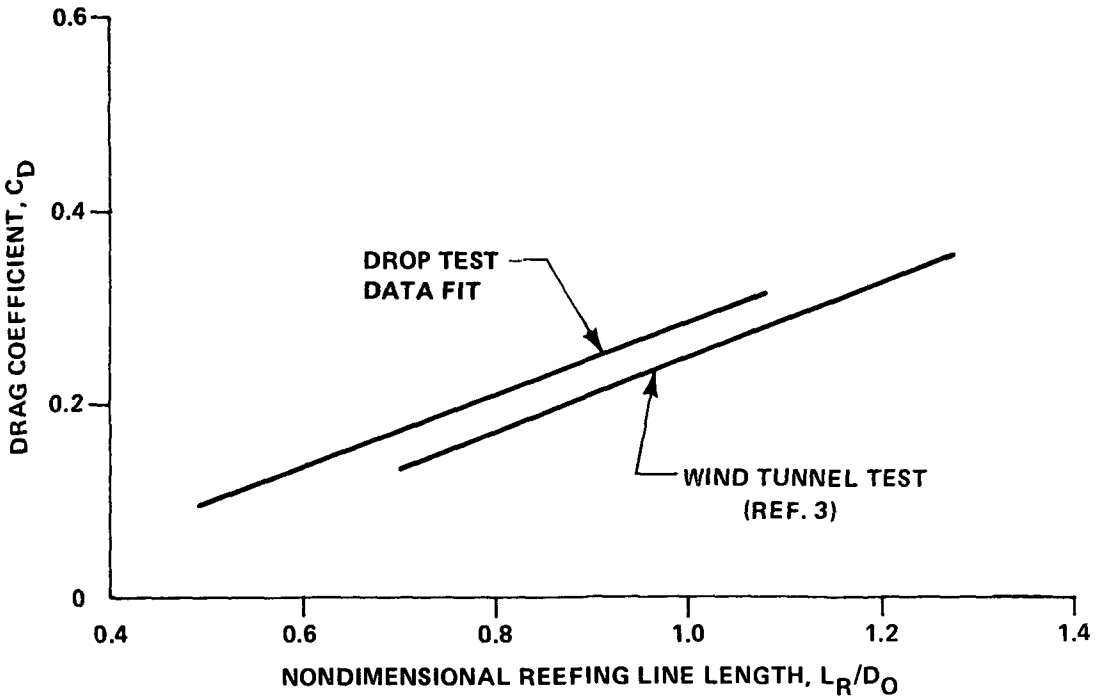

Figure 4-9. MAIN CHUTES CLUSTER REEFED DRAG COEFFICIENT

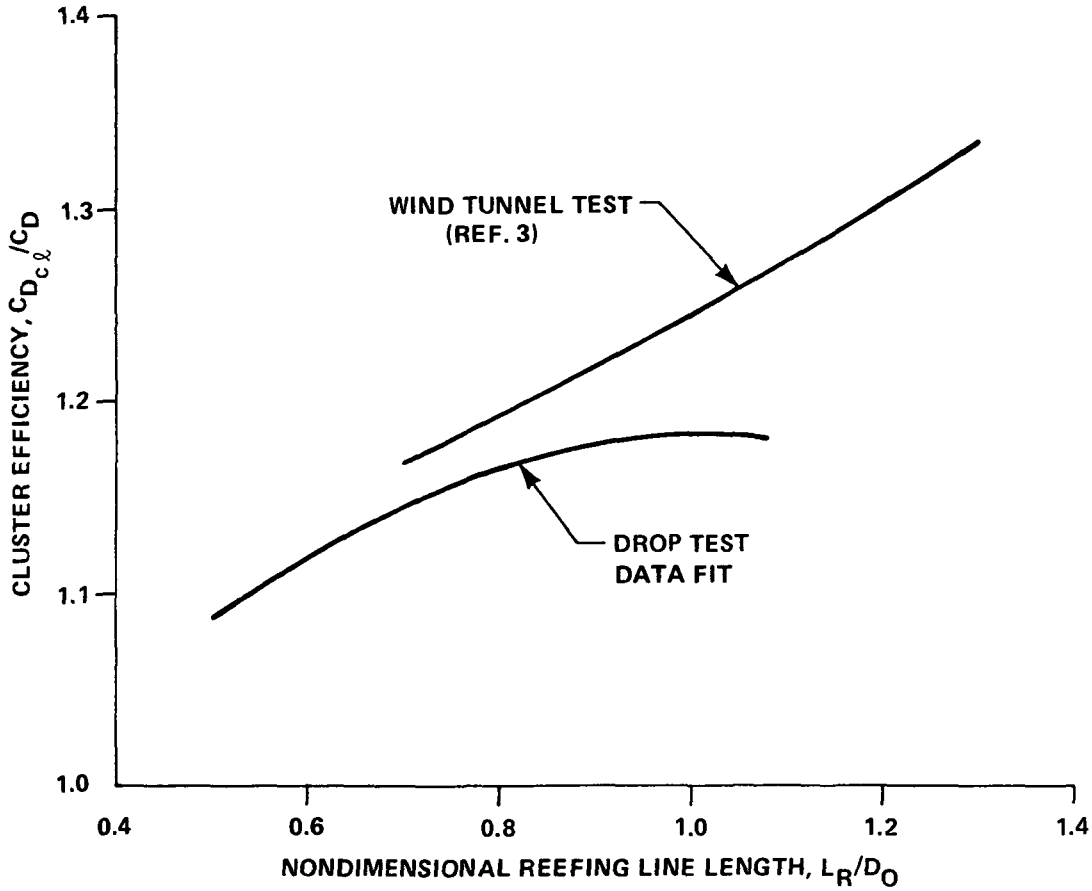

Figure 4-10. REEFED MAIN CHUTES CLUSTER EFFICIENCY FACTOR

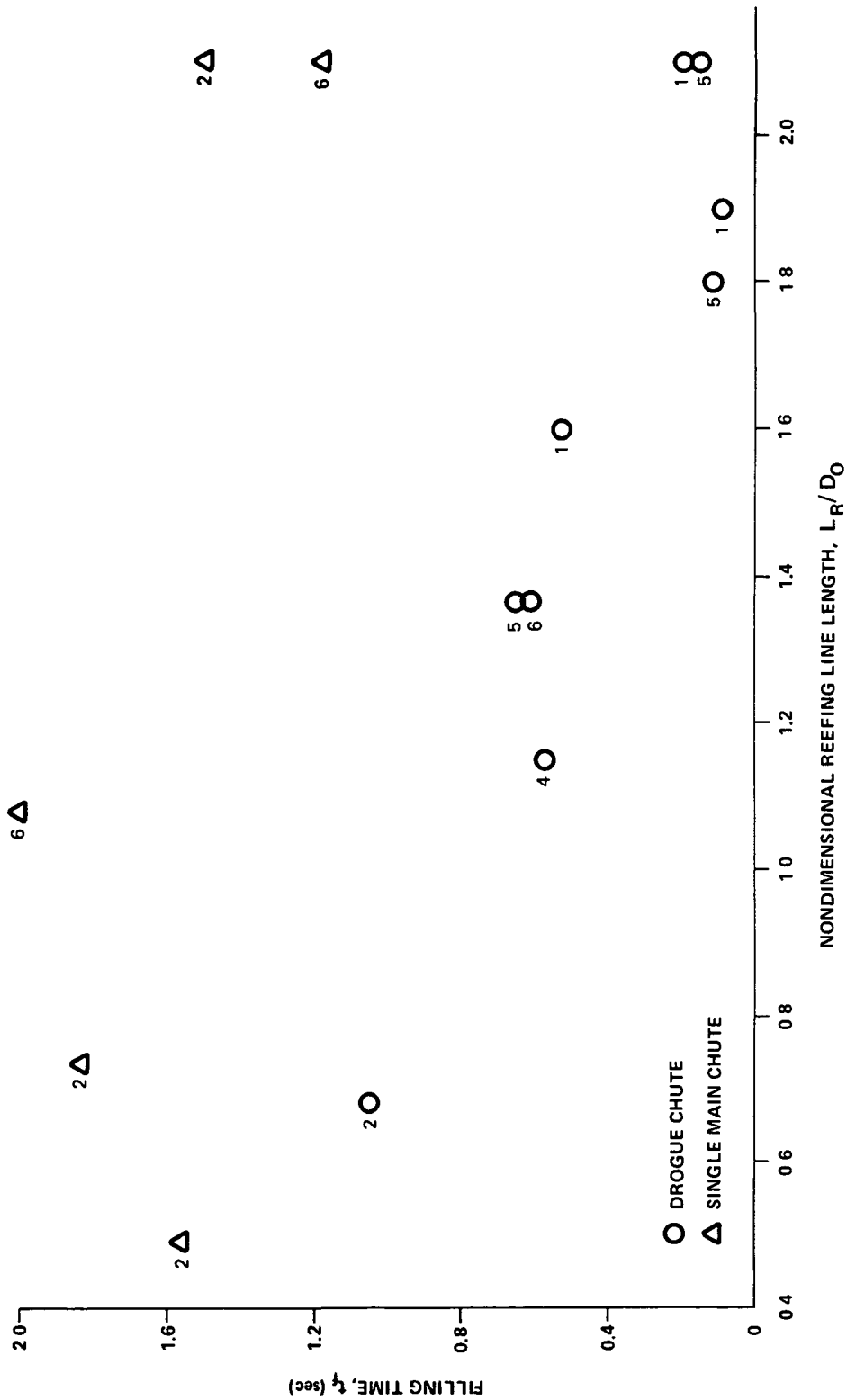

Figure 4-11. FILLING TIME OF DSS PARACHUTES VERSUS NONDIMENSIONAL REEFING LINE LENGTH

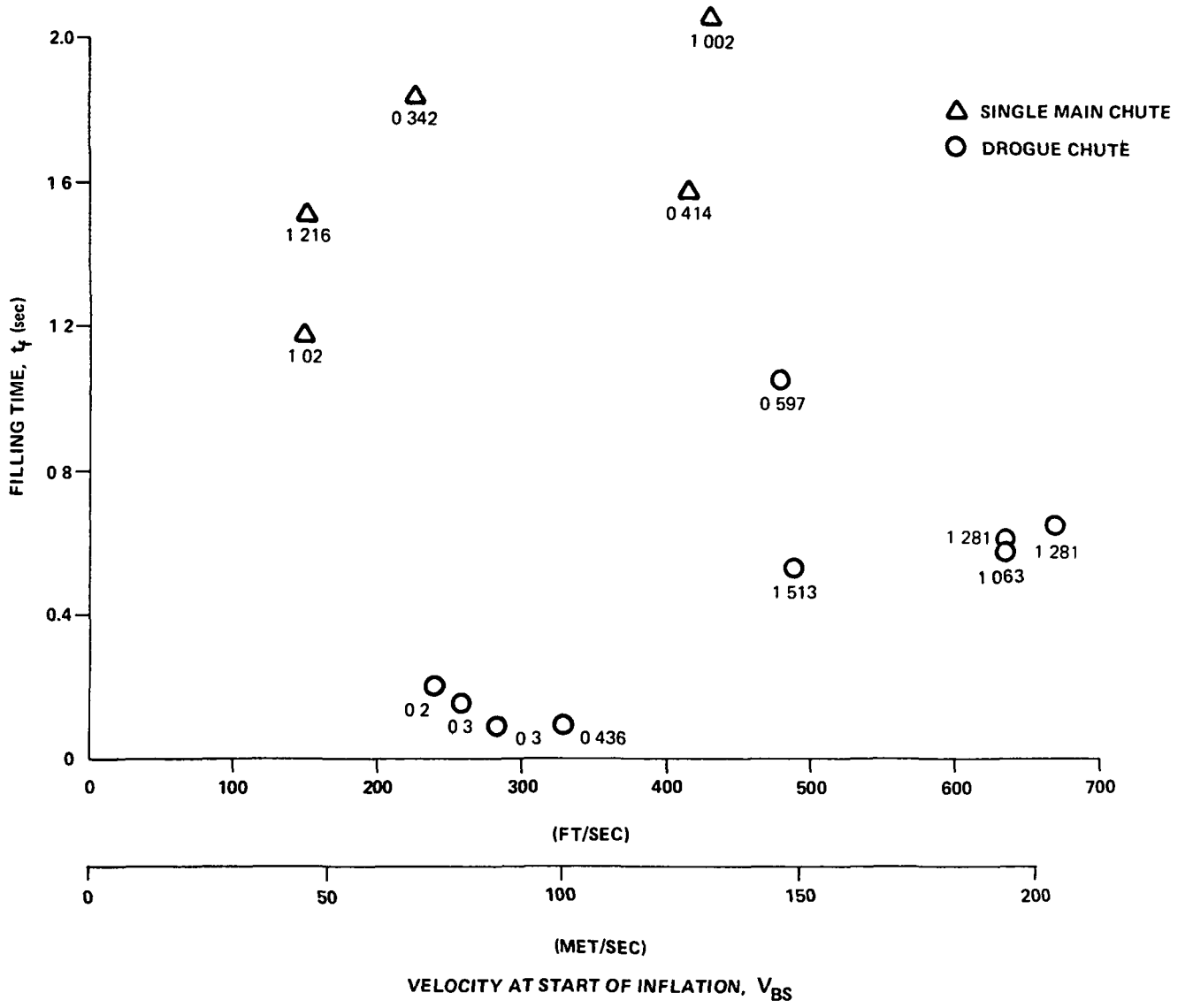

Figure 4-12. FILLING TIME OF DSS PARACHUTES VERSUS VELOCITY

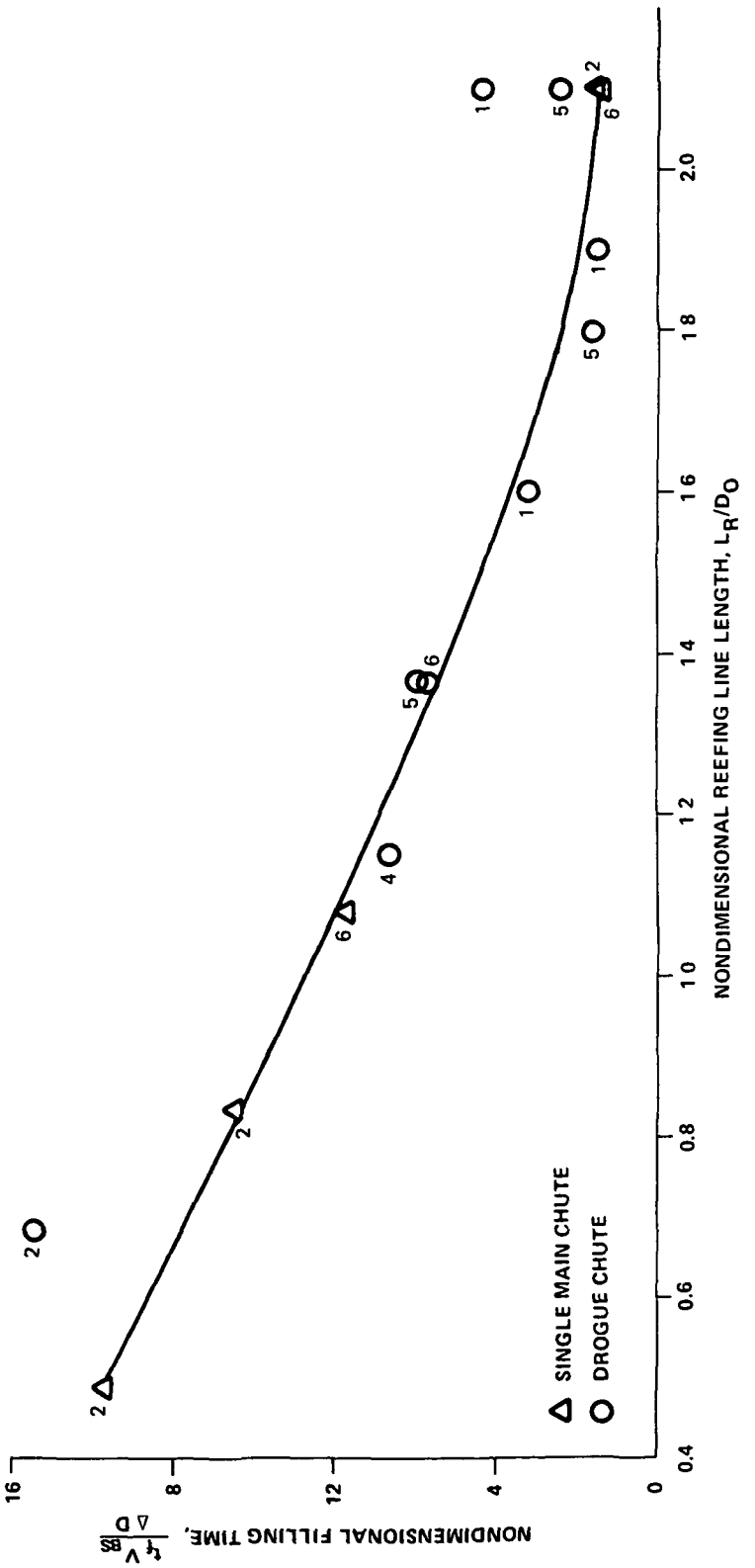

Figure 4-13. NONDIMENSIONAL FILLING TIME OF THE DSS PARACHUTES

Page intentionally left blank

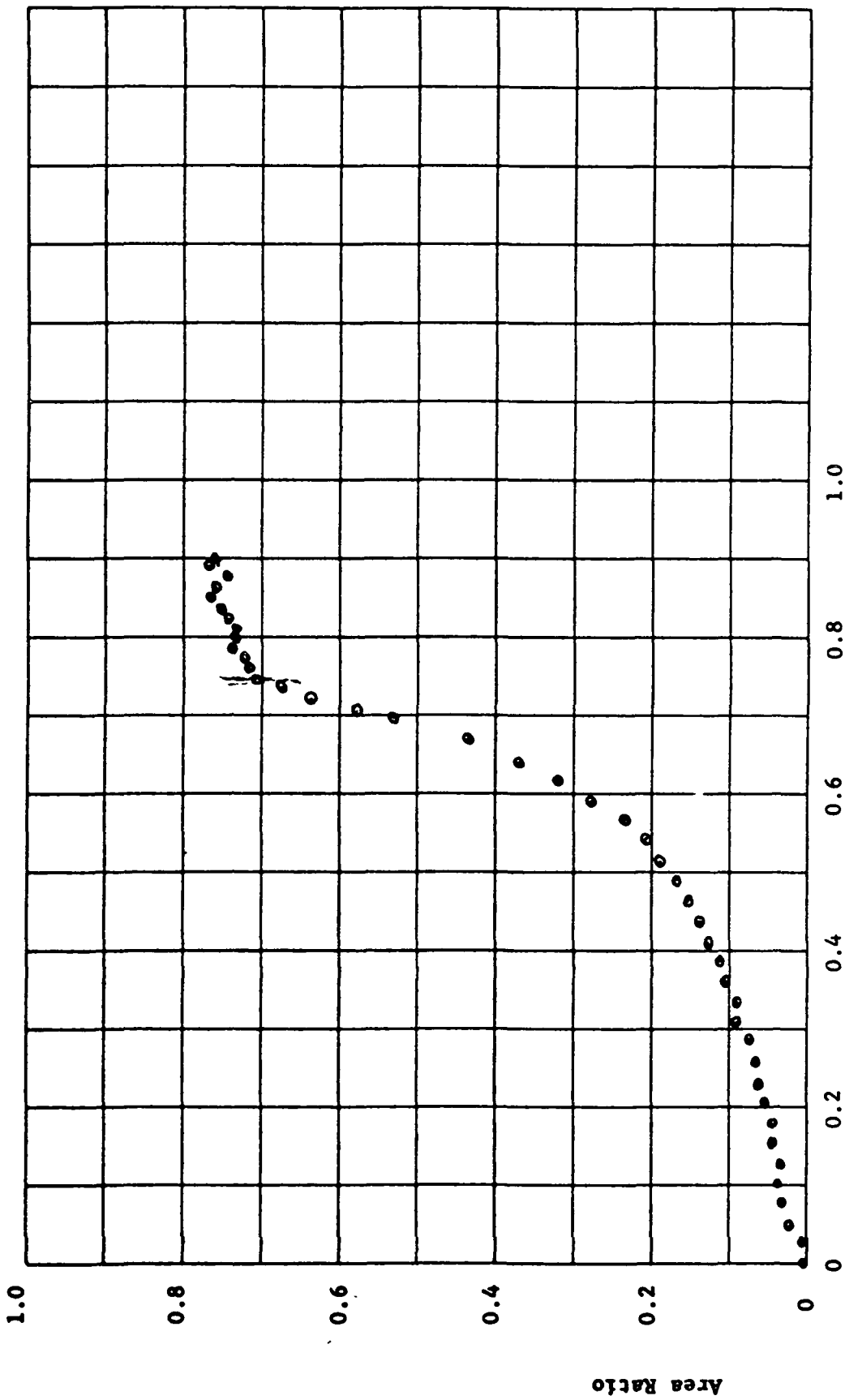

Figure 4-14. DAD-1 DROGUE 1st REEF AREA BUILDUP

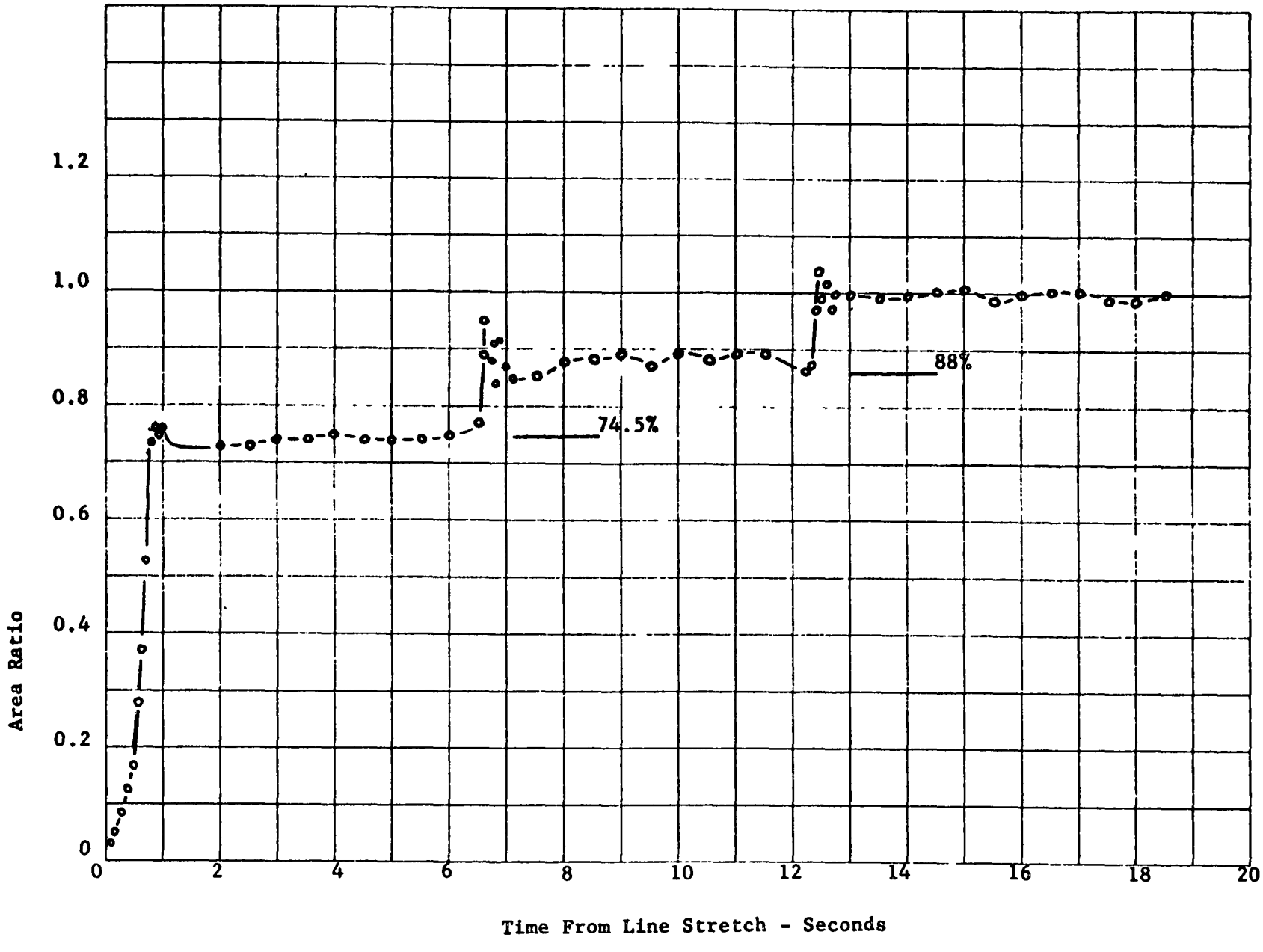

Figure 4-15. DAD-1 DROGUE PARACHUTE AREA BUILDUP

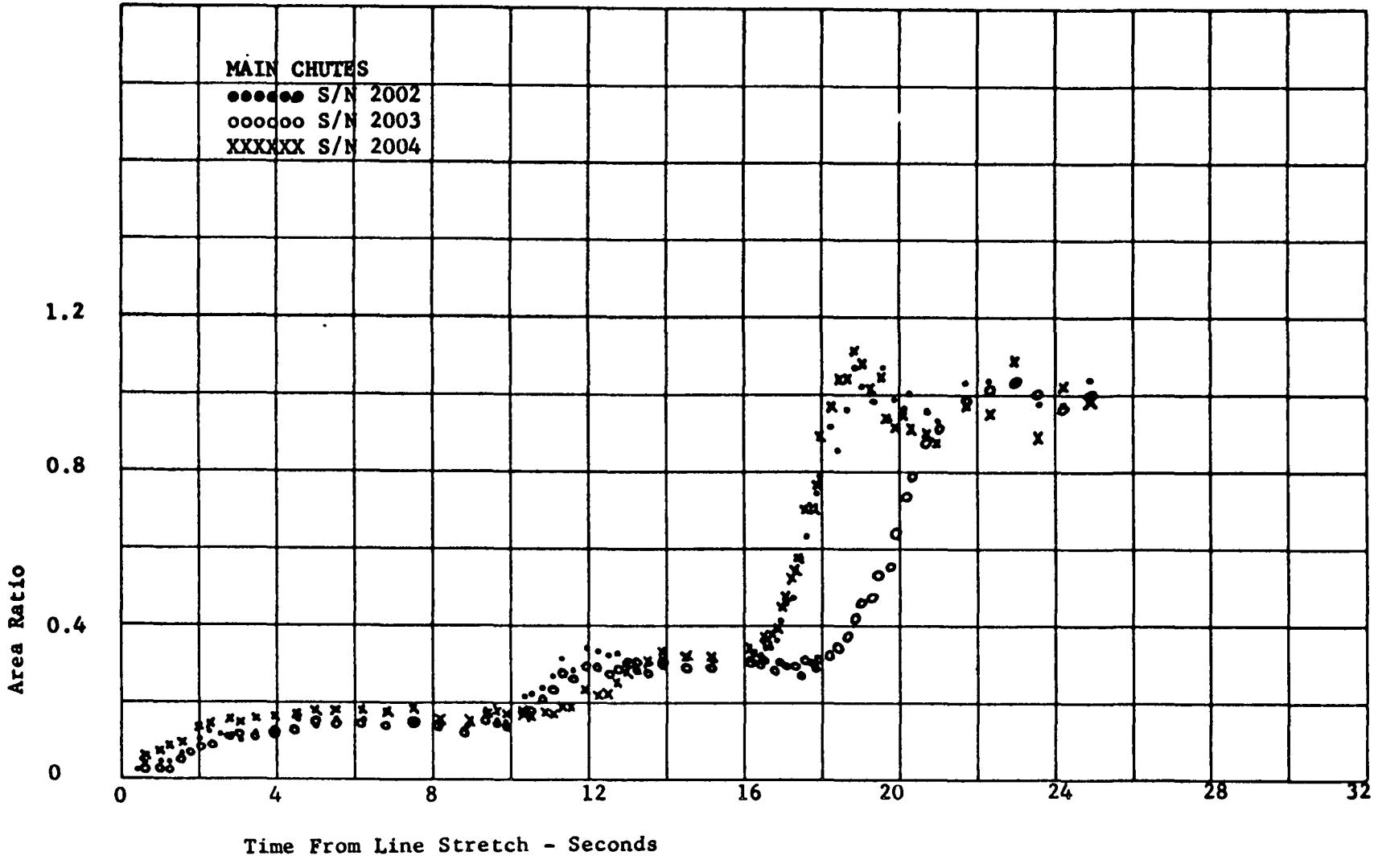

Figure 4-16. DAD-1 MAIN PARACHUTES AREA BUILDUP

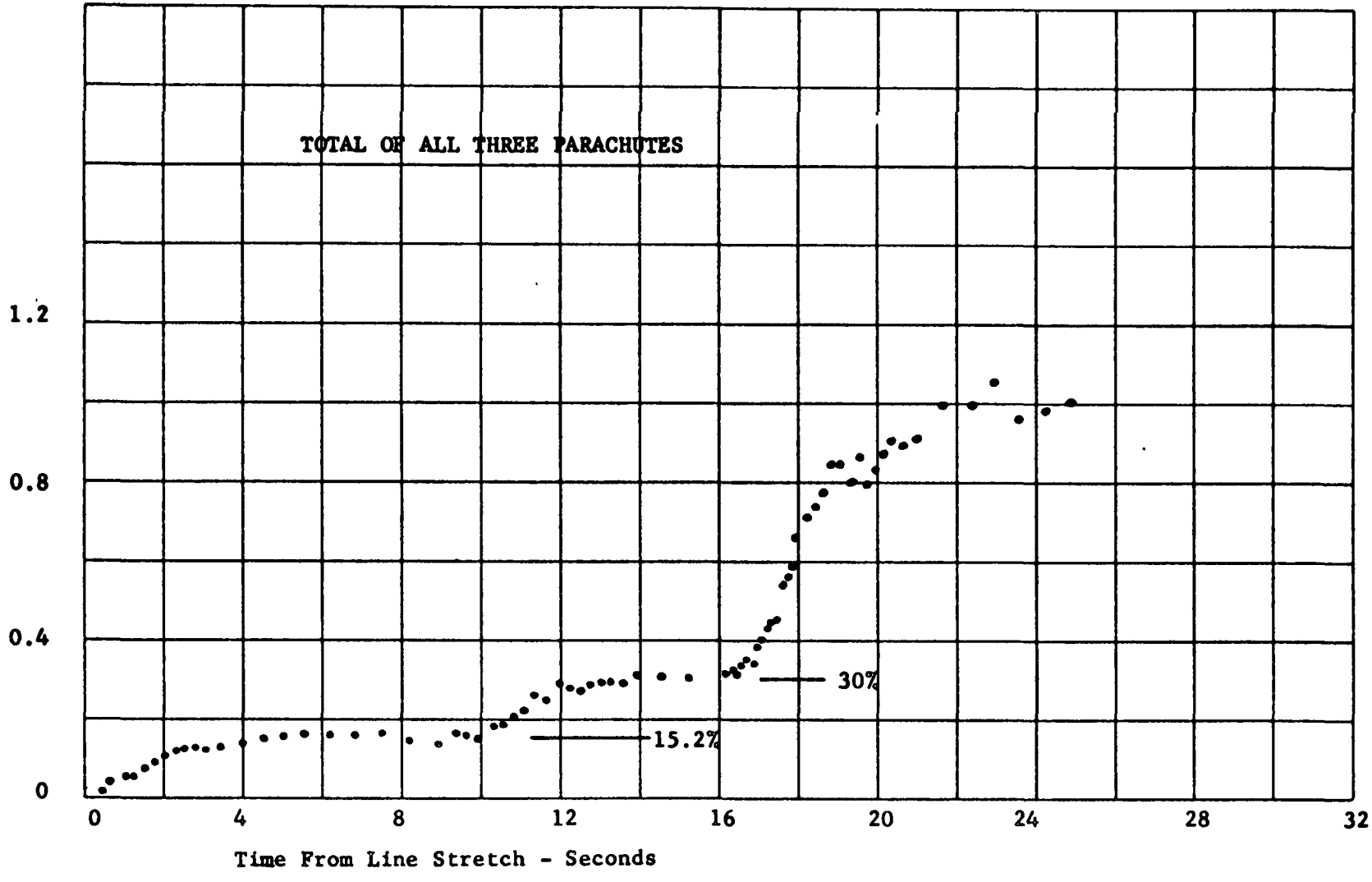

Figure 4-17. DAD-1 TOTAL MAIN PARACHUTES AREA BUILDUP

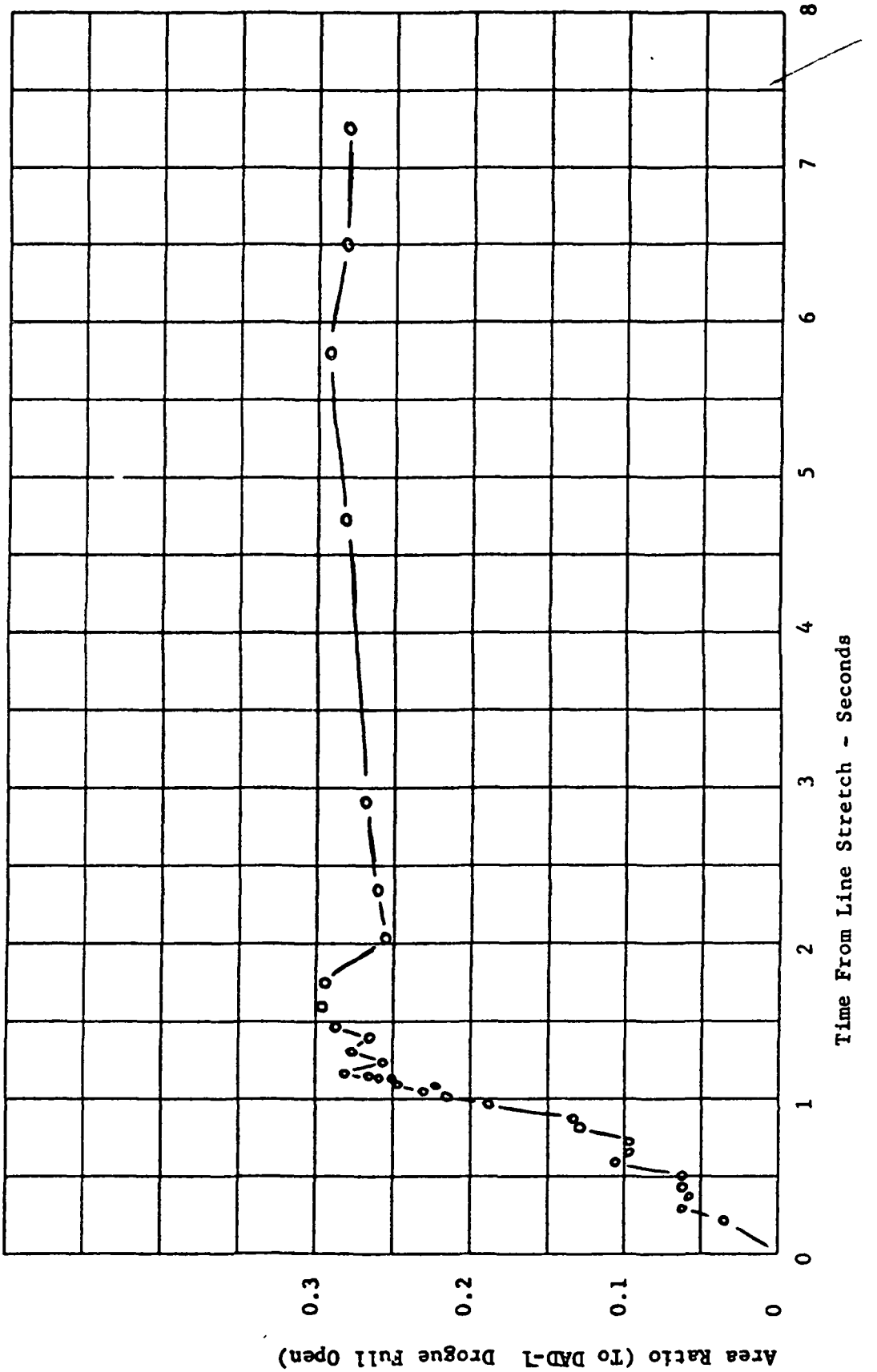

Figure 4-18. DAD-2 DROGUE AREA BUILDUP

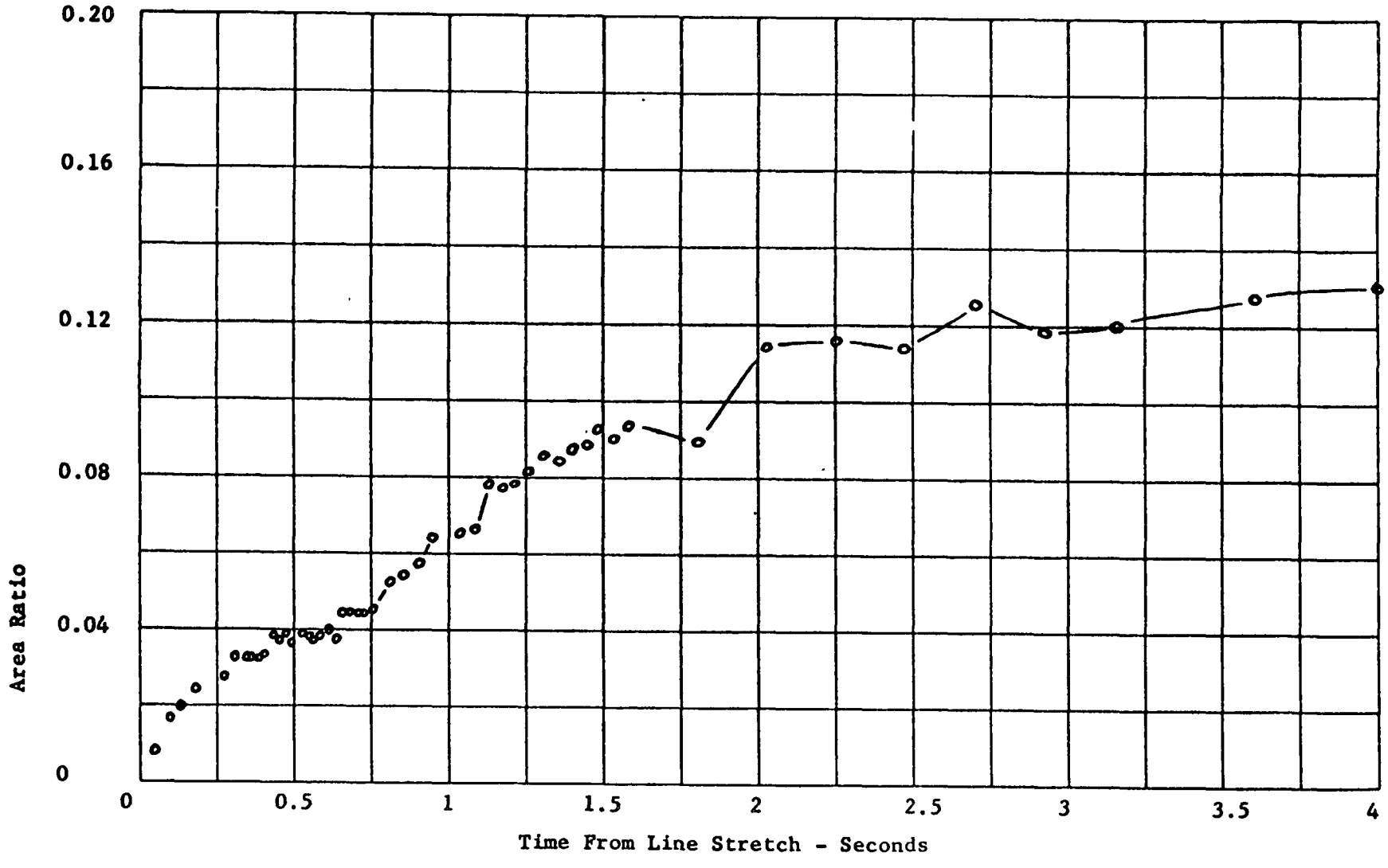

Figure 4-19. DAD-2 MAIN PARACHUTE AREA BUILDUP TO 1st REEF

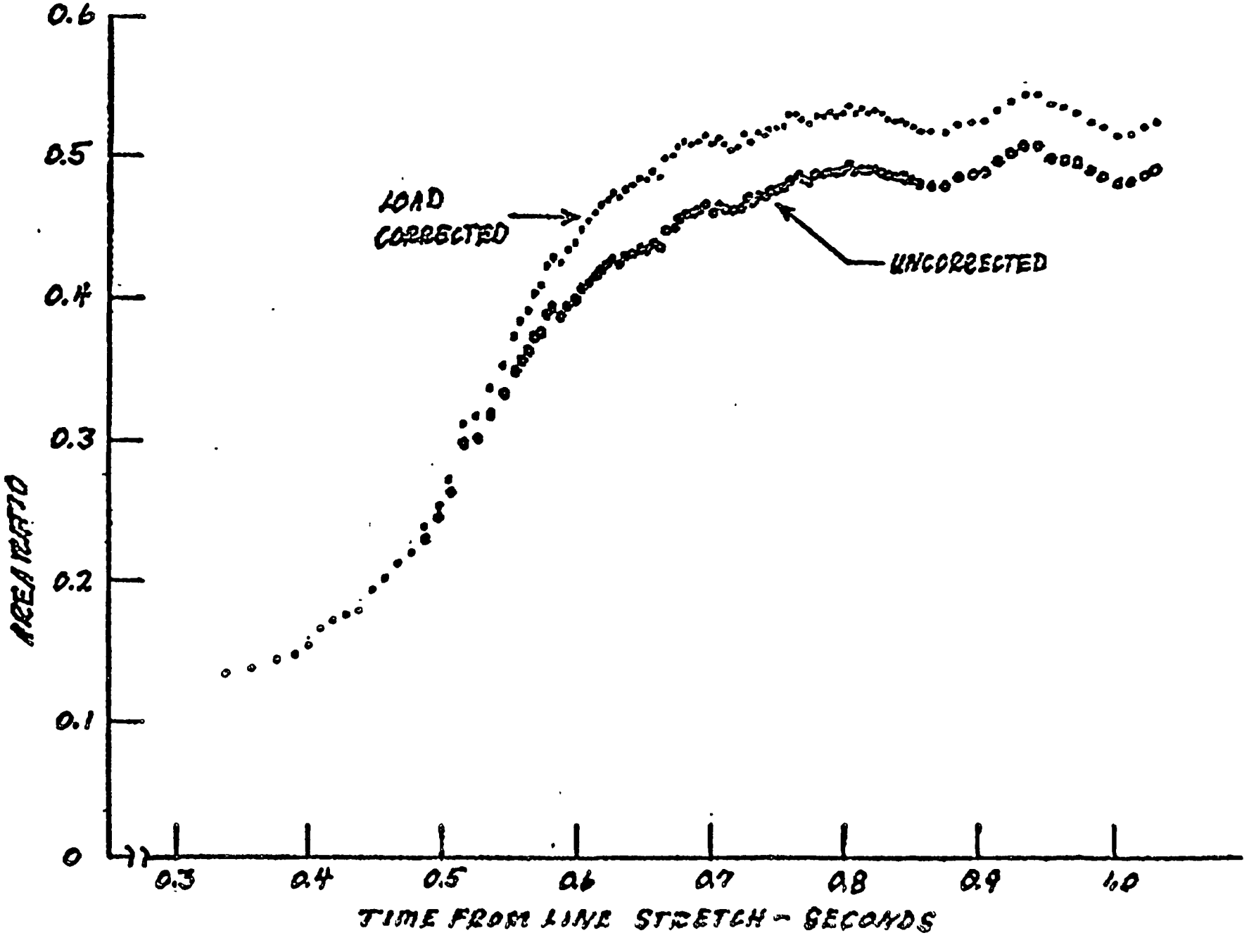

Figure 4-20. DAD-4 DROGUE AREA BUILDUP CURVE

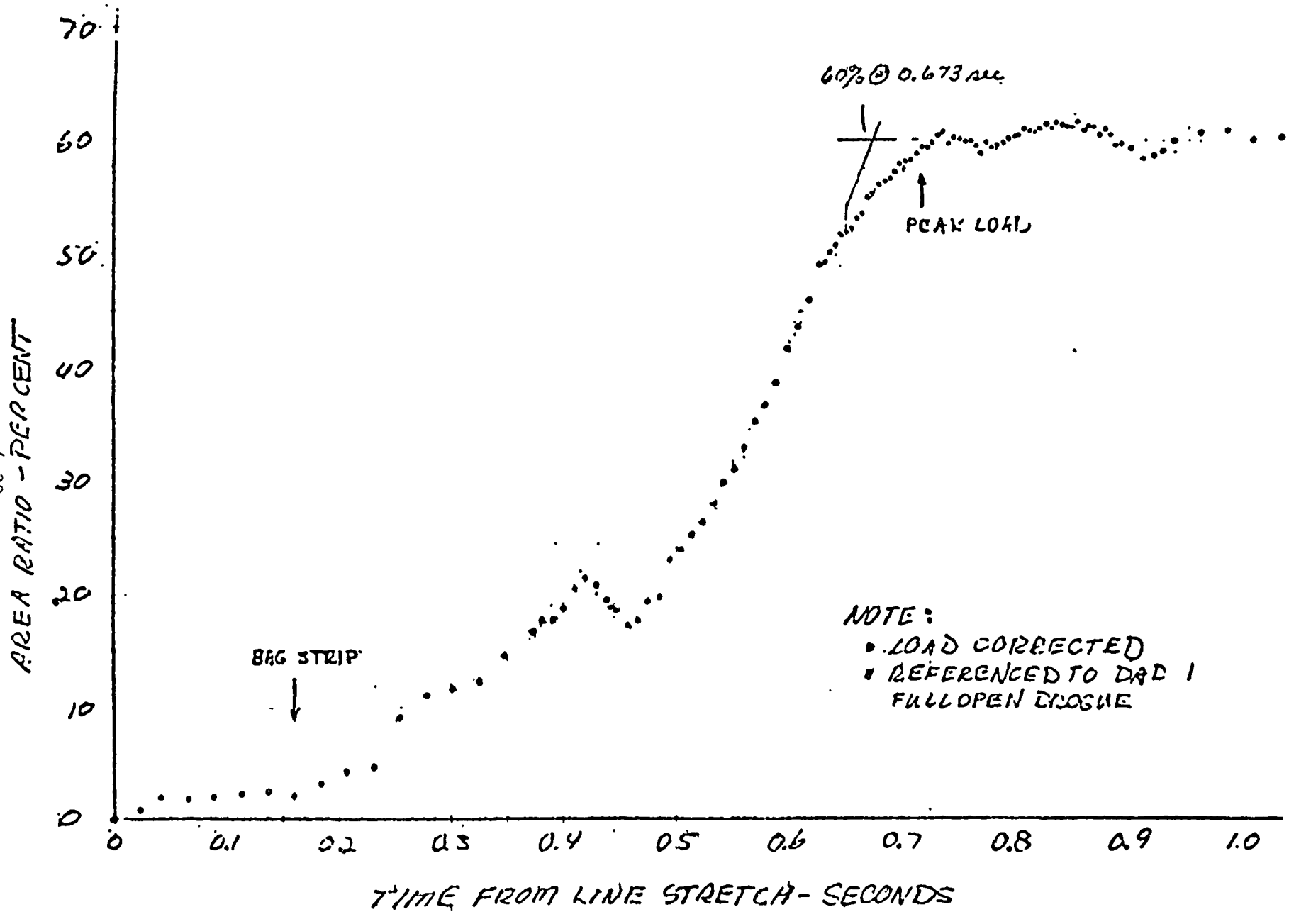

Figure 4-21. DAD-6 DROGUE CHUTE AREA BUILDUP

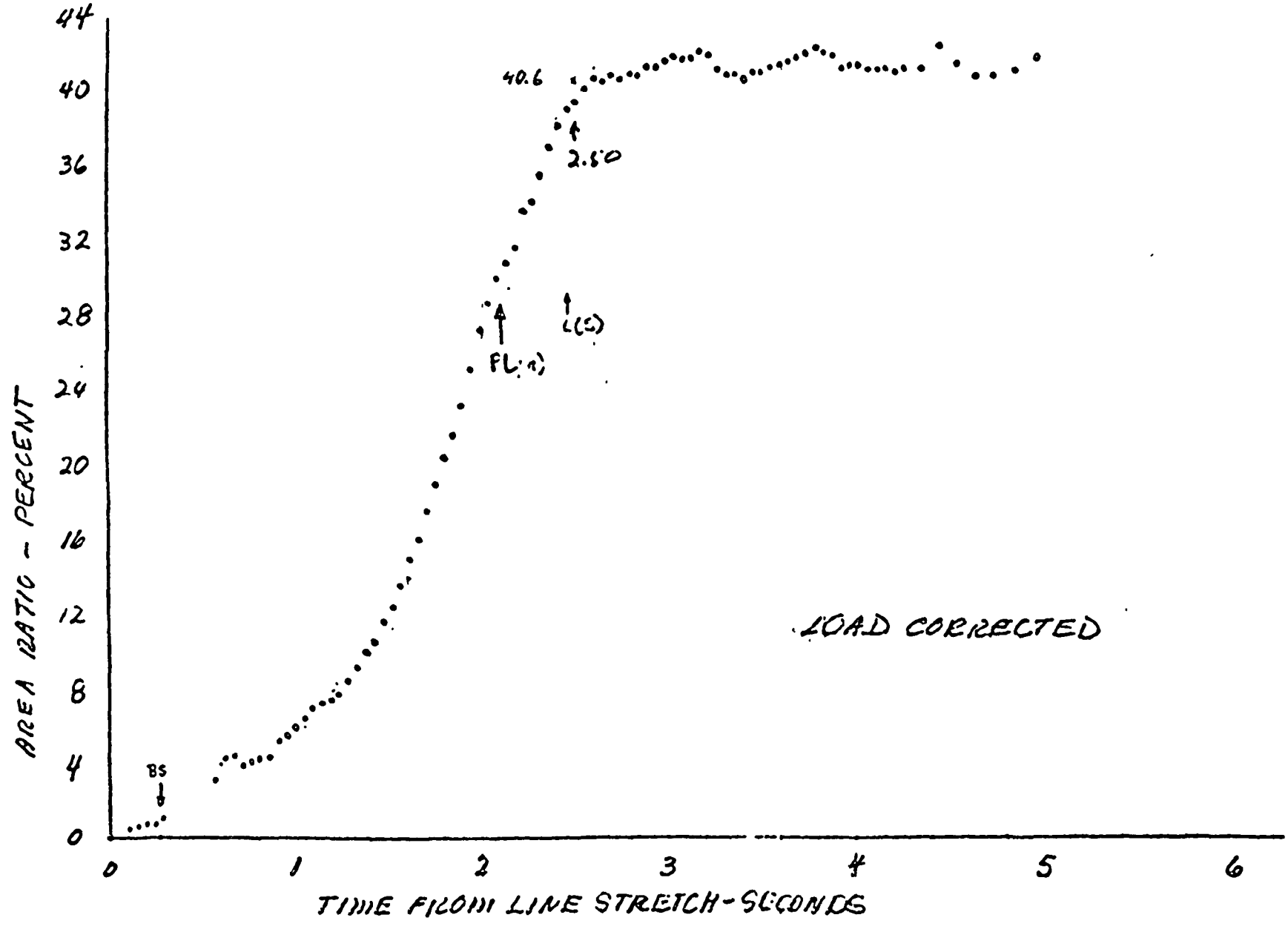

Figure 4-22. DAD-6 MAIN CHUTE AREA BUILDUP

Section V

CONCLUSIONS

The full open and the reefed drag performance of the DSS drogue chute agreed well with the wind tunnel test results and the predictions made there from.

The drop test data was too limited to isolate cluster interference from the single main chute drag performance. In the full open case the drag degradation due to cluster interference was observed to be about seven percent whereas, the single main chute drag performance agreed well with the predicted results. However, in the reefed case the main chute cluster drag coefficients were higher than the single chute data as observed in a previous wind tunnel test.

A simultaneous extraction of the main chute cluster was achieved in the cluster tests. The blanketing effect of the lead parachutes on the lag parachute in a cluster was not evidenced. However, non-synchronous firing of the reefing line cutters resulted in non-synchronous opening in the second reef stages and full open conditions.

The main chutes were generally slow in reaching a steady state for all stages of inflation. The filling time data was obtained and was nondimensionalized to aid in the prediction of filling times for the SRB flight cases.

A uniform and orderly deployment of the DSS parachutes was achieved in the DTV flight altitude and dynamic pressure environment. Critical values of the drogue chute drag to weight ratio were estimated to prevent line sail on the drogue chute or on inflation overtake on the main chute cluster.

Section VI

RECOMMENDATIONS

The drag performance estimates of the prototype SRB parachutes were made based on limited drop test data. The variation of the parachute drag coefficients from the averaged values is required to calculate parachute load levels during reefed stages, and the range of water impact velocities under terminal conditions. It is, therefore, recommended that a study be conducted to determine tolerance levels on the estimated parachute performance.

Section VII

REFERENCES

1. Vickers, J. R. and Mickey, F. E., "Wind Tunnel Test Report, SRB Drogue Parachute System", Northrop Corporation, Ventura Division, NVR 74-45, December 1974.

2. Utreja, L. R., "SRB Drogue Chute Deployment Test Report", Northrop Services, Inc., Huntsville, TR-230-1690, July 1976.

3. Utreja, L. R., "Wind Tunnel Drag Test Report on the Solid Rocket Booster Parachute System", Northrop Services, Inc., Huntsville, TR-230-1666, July 1976.

4. Bacchus, D. L., "Aerodynamic Performance Analysis of DSS Parachutes", Aerophysics Division, System Dynamics Laboratory, MSFC, ED32-76-87, October 1976.

5. Utreja, L. R., "SA38F Wind Tunnel Test Data Analysis", Northrop Services, Inc., Huntsville, M-9230-76-74, December 1976.

6. Utreja, L. R., "SRB Nose Cap Ejection Rocket Sled Tests Analysis", Northrop Services, Inc., Huntsville, M-9224A-78-16, May 1978.

7. Bacon, R. K., "Drop Test Plan for Space Shuttle Program Solid Rocket Booster Deceleration Subsystem", Martin Marietta Corporation, SRB-DSS-TM06, May 1977.

8. Moog, R. D., et al, "Drop Test Report for Solid Rocket Booster Decelerator Subsystem Development Air Drop Nos. 1 and 2", Martin Marietta Corporation, SRB-DSS-TM11-1, November 1977.

9. Martin Marietta Corporation, Informal Transmittals to MSFC.